

Provided for non-commercial research and education use.  
Not for reproduction, distribution or commercial use.



This article appeared in a journal published by Elsevier. The attached copy is furnished to the author for internal non-commercial research and education use, including for instruction at the authors institution and sharing with colleagues.

Other uses, including reproduction and distribution, or selling or licensing copies, or posting to personal, institutional or third party websites are prohibited.

In most cases authors are permitted to post their version of the article (e.g. in Word or Tex form) to their personal website or institutional repository. Authors requiring further information regarding Elsevier's archiving and manuscript policies are encouraged to visit:

<http://www.elsevier.com/copyright>



Contents lists available at ScienceDirect

## Journal of South American Earth Sciences

journal homepage: [www.elsevier.com/locate/jsames](http://www.elsevier.com/locate/jsames)

## The Arequipa Massif of Peru: New SHRIMP and isotope constraints on a Paleoproterozoic inlier in the Grenvillian orogen

C. Casquet<sup>a,\*</sup>, C.M. Fanning<sup>b</sup>, C. Galindo<sup>a</sup>, R.J. Pankhurst<sup>c</sup>, C.W. Rapela<sup>d</sup>, P. Torres<sup>e</sup>

<sup>a</sup>Dpto. Petrología y Geoquímica, Fac.Ciencias Geológicas, Inst. Geología Económica (CSIC, Universidad Complutense), 28040 Madrid, Spain

<sup>b</sup>Research School of Earth Sciences, The Australian National University, Canberra, ACT 200, Australia

<sup>c</sup>British Geological Survey, Keyworth, Nottingham NG12 5GG, UK

<sup>d</sup>Centro de Investigaciones Geológicas, Universidad de La Plata, 1900 La Plata, Argentina

<sup>e</sup>Universidad Nacional de Ingeniería, Av. Tupac Amaru 210, Lima, Peru

### ARTICLE INFO

#### Article history:

Received 20 February 2009

Accepted 23 August 2009

#### Keywords:

Arequipa Massif

Grenvillian orogeny

Paleoproterozoic

U–Pb SHRIMP zircon dating

Rodinia

### ABSTRACT

The enigmatic Arequipa Massif of southwestern Peru is an outcrop of Andean basement that underwent Grenville-age metamorphism, and as such it is important for the better constraint of Laurentia–Amazonia ties in Rodinia reconstruction models. U–Pb SHRIMP zircon dating has yielded new evidence on the evolution of the Massif between Middle Paleoproterozoic and Early Paleozoic. The oldest rock-forming events occurred in major orogenic events between *ca.* 1.79 and 2.1 Ga (Orosirian to Rhyacian), involving early magmatism (1.89–2.1 Ga, presumably emplaced through partly Archean continental crust), sedimentation of a thick sequence of terrigenous sediments, UHT metamorphism at *ca.* 1.87 Ga, and late felsic magmatism at *ca.* 1.79 Ga. The Atico sedimentary basin developed in the Late-Mesoproterozoic and detrital zircons were fed from a source area similar to the high-grade Paleoproterozoic basement, but also from an unknown source that provided Mesoproterozoic zircons of 1200–1600 Ma. The Grenville-age metamorphism was of low-*P* type; it both reworked the Paleoproterozoic rocks and also affected the Atico sedimentary rocks. Metamorphism was diachronous: *ca.* 1040 Ma in the Quilca and Camaná areas and in the San Juan Marcona domain, 940 ± 6 Ma in the Mollendo area, and between 1000 and 850 Ma in the Atico domain. These metamorphic domains are probably tectonically juxtaposed. Comparison with coeval Grenvillian processes in Laurentia and in southern Amazonia raises the possibility that Grenvillian metamorphism in the Arequipa Massif resulted from extension and not from collision. The Arequipa Massif experienced Ordovician–Silurian magmatism at *ca.* 465 Ma, including anorthosites formerly considered to be Grenvillian, and high-*T* metamorphism deep within the magmatic arc. Focused retrogression along shear zones or unconformities took place between 430 and 440 Ma.

© 2009 Elsevier Ltd. All rights reserved.

### 1. Introduction

The Arequipa Massif (Cobbing and Pitcher, 1972; Shackleton et al., 1979) is an outcrop of metamorphic rocks and cross-cutting batholiths at least 800 km long and 100 km wide, along the desert coast of southern Peru, between the Andean Cordillera and the Chile–Peru trench (Fig. 1). It is part of the Andean basement that crops out both as discontinuous inliers throughout the belt and in uplifted blocks in the Andean foreland, from as far north as Venezuela to as far south as the Sierras Pampeanas of Argentina (e.g., Ramos, 2008). Metamorphic rocks of the Arequipa Massif are mostly metasedimentary and range from amphibolite to granulite facies. Pervasive retrogression under greenschist-facies was focused within late strongly sheared zones. Early dating of granulites between Camaná and Mollendo (Fig. 1) by Rb–Sr

(whole-rock isochrons) and U–Pb (bulk dating of zircons) first resulted in Precambrian ages of *ca.* 1.8–1.95 Ga (Cobbing et al., 1977; Dalmayrac et al., 1977; Shackleton et al., 1979). Regional metamorphism in the Arequipa Massif according to these authors resulted from a single Paleoproterozoic tectonothermal event; the age of sedimentary protoliths was estimated at *ca.* 2.0 Ga. Emplacement of plutons and metamorphic reworking under low-grade conditions took place in the Paleozoic at *ca.* 450 Ma and *ca.* 390 Ma (Shackleton et al., 1979).

Paleogeographic models of Proterozoic continents as developed in the 1990s led to a renewed interest in the study of the Arequipa Massif. According to these models most continental masses were united into a large supercontinent called Rodinia by the end of the Mesoproterozoic as a result of the Grenvillian orogeny (e.g. Moores, 1991; Hoffman, 1991). In Hoffman's model, and in more recent paleogeographical reconstructions, the Amazonian craton appears juxtaposed to Laurentia (the ancestral North America craton) at *ca.* 1.0 Ga, although their relative positions vary from one

\* Corresponding author. Tel.: +34 913944908; fax: +34 915442535.

E-mail address: [casquet@geo.ucm.es](mailto:casquet@geo.ucm.es) (C. Casquet).

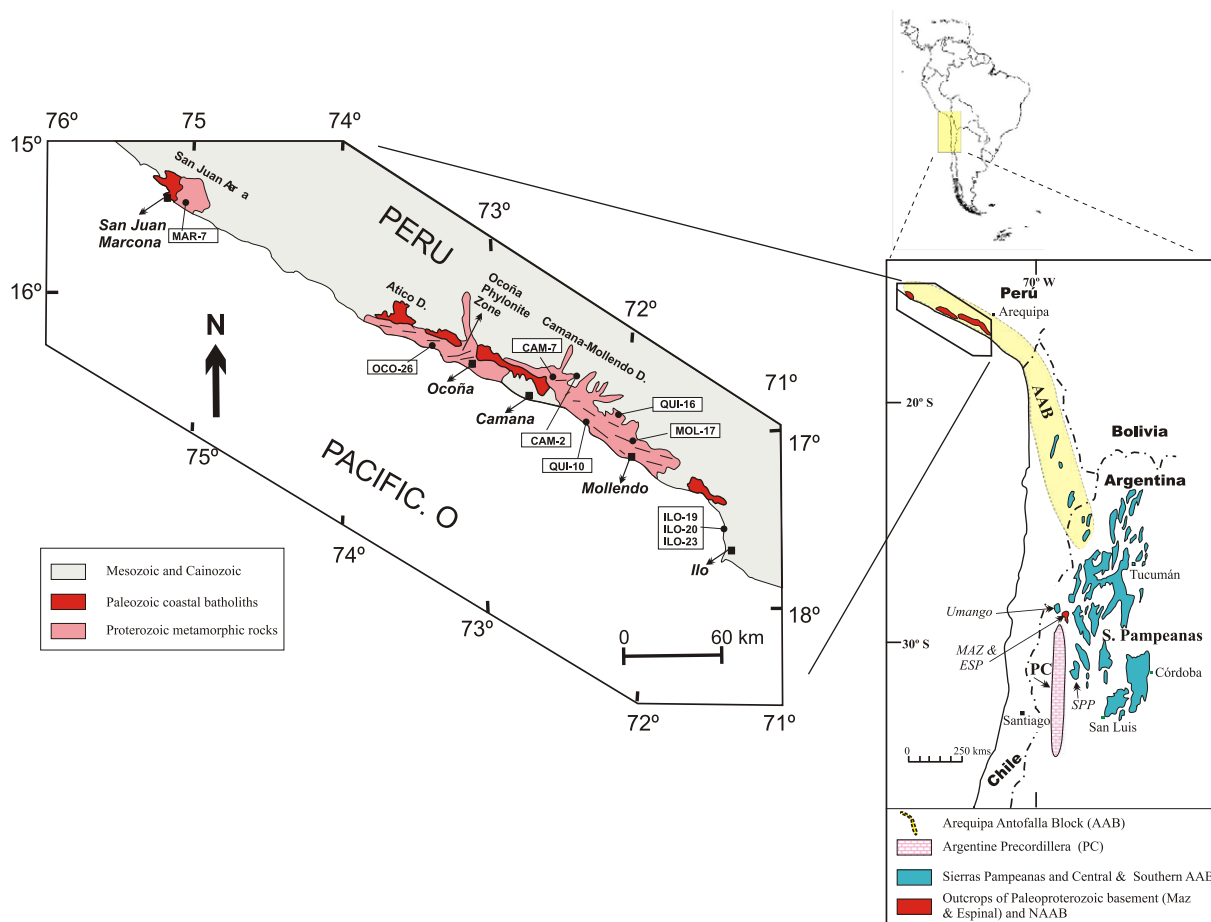


**Fig. 1.** Sketch map of the Arequipa Massif showing domains distinguished in the text and location of samples. Insets show the location of the Arequipa Massif in South America and relationships with other pre-Andean outcrops in Northern Chile and Argentina.

version to another (e.g., Dalla Salda et al., 1992; Dalziel, 1994, 1997; Sadowski and Bettencourt, 1996; Sadowski, 2002; Loewy et al., 2003; Tohver et al., 2004; Li et al., 2008). Amazonia broke away from Laurentia in the Neoproterozoic, leading to the opening of the Iapetus Ocean, and the intervening Grenvillian orogen broke into conjugate belts along the margins of the rifted continents. Because Grenvillian ages were known from elsewhere in South America, lending credence to the Laurentia–Amazonia connection in this way, the age, paleogeography and tectonics of the Arequipa Massif became the subject of thorough isotope (Nd and Pb) and renewed geochronological research (Wasteneys et al., 1995; Tosdal, 1996; Bock et al., 2000; Loewy et al., 2003, 2004).

U–Pb single-grain zircon dating of granulites yielded Grenvillian ages for the high-grade metamorphism of ca. 1200 Ma near Quilca, and ca. 970 Ma near Mollendo, with protolith ages of ca. 1.9 Ga (Wasteneys et al., 1995). The age of regional metamorphism in the Arequipa Massif was thus switched from Paleoproterozoic to Late-Mesoproterozoic and the Massif was re-interpreted as having originated within the Grenville province. Further conventional zircon U–Pb dating was carried out by Loewy et al. (2004) on igneous gneisses of the San Juan and Mollendo areas. They inferred a complex history of crystallization of protoliths between 1851 and 1818 Ma, and at ca. 1790 Ma, with development of an earlier gneissic fabric (M1 metamorphism) prior to the latter event. Grenville-age metamorphism (M2) took place at ca. 1052 Ma at San Juan and 935 Ma near Mollendo, suggesting a north-to-south younging of the metamorphic peak. A retrograde metamorphic overprint (M3) and conspicuous granite magmatism took place in the Ordovician

at ca. 465 Ma (Loewy et al., 2003). Martignole and Martelat (2003) focused on the structure, geochronology and mineralogy of the high-grade metamorphism between Camaná and Mollendo, which they classified as of the UHT type ( $T > 900$  °C; 1.0–1.3 GPa) on account of ubiquitous peak assemblages with orthopyroxene + sillimanite + quartz and the local coexistence of sapphirine + quartz. They attempted to date this metamorphism by *in situ* chemical (CHIME) U–Th–Pb determinations on monazites; the calculated ages range from 1064 to 956 ( $\pm 50$ ) Ma, with a peak ca. 1.0 Ga.

The Arequipa Massif has long been considered to be the northern exposure of a larger hypothetical continental block that crops out as basement inliers within the Andean Cordillera in northern Chile and Northern Argentina, i.e., the composite Arequipa–Antofalla craton (Ramos, 1988). This block includes a Grenvillian basement with post-Grenvillian metamorphic and igneous overprints as young as 0.4 Ga (Loewy et al., 2003). Isotope (Nd and Pb) and geochronological considerations led Casquet et al. (2008) to establish comparisons between the Arequipa Massif and Grenvillian terranes recognized in the Western Sierras Pampeanas of NW Argentina, i.e., the Andean foreland, thus enlarging the boundaries of the Arequipa–Antofalla block. However, both the role of the Arequipa–Antofalla block in the Grenvillian orogeny and its pre-Grenvillian history are still poorly known. Based on similarities in 1.8–1.0 Ga basement rocks and pre-rift glacial sedimentary cover sequences, Dalziel (1992, 1994) proposed that the Arequipa Massif was the tip of a promontory of NE Laurentia that was accreted to Amazonia during the Grenvillian orogeny. Sadowski and Betten-

court (1996, and references therein) proposed a similar paleogeography. However, further testing of the hypothesis and new Pb-isotope composition evidence led to an alternative postulated source for the Arequipa–Antofalla craton in the Kalahari craton (Loewy et al., 2003). According to Loewy et al. (2004) docking of the orphaned allochthonous Arequipa–Antofalla craton to Amazonia took place at ca. 1.04 Ga during the Sunsás orogeny, a Grenville-age tectonic event long recognized in SE Bolivia and along the SW margin of Amazonia in Brazil (Litherland et al., 1989; Cordani and Teixeira, 2007, among others).

It is now widely accepted that the Grenvillian orogeny played an important role in Central Andean South America, as evidenced by the Arequipa Massif and the Western Sierras Pampeanas (e.g., Rapela et al., this volume). Moreover Grenville-age rocks have long been recognized in the basement of the Northern Andes (e.g., Restrepo-Pace et al., 1997; Cordani et al., 2005b) and along the southern margin of the Amazonian craton (Cordani and Teixeira, 2007). However the pre-Grenvillian history and the time and mode of accretion of the Grenvillian terranes to nearby Amazonia, and correlations with the alleged Laurentian conjugate margin, still remain speculative.

This contribution is aimed at better constraining the igneous and metamorphic history of the Arequipa Massif by means of new U–Pb SHRIMP determinations and complementary geochemical evidence. We conclude that the Massif was the site of a complex history that consisted of sedimentation, magmatism and metamorphism (UHT) in the Paleoproterozoic, development of a sedimentary basin in the Mesoproterozoic, Grenville-age medium- to high-grade metamorphism, and local metamorphic reworking and magmatism in the Early Paleozoic.

## 2. Geological setting

The most comprehensive geological description of the Arequipa Massif is that of Shackleton et al. (1979). We retain here some of the domains that they distinguished to better locate our samples. A summary description follows, based on their work and our own observations.

### 2.1. The northern section

The *San Juan Marcona area* in the north (Fig. 1) consists of a basement and a discordant cover sequence. The latter is formed by glacial diamictites of the Chiquerio formation followed by a carbonate cap, the San Juan formation, both probably Neoproterozoic (Chew et al., 2007). The basement consists of banded migmatitic gneisses and minor fine-grained gneisses, strongly dismembered concordant pegmatites, concordant and discordant amphibolite dykes, and foliated megacrystic granite of ca. 1790 Ma (Loewy et al., 2003). Late granitic plutons cutting the discordance are Ordovician (Loewy et al., 2003). The *Atico domain*, between Atico and Ocoña is medium-grade, with staurolite (+andalusite; Shackleton et al., 1979) schists, grey metasandstones, variably retrogressed amphibolites and concordant pegmatite sheets. Southward, this domain merges into a low-grade zone, the *Ocoña phyllonite zone* that consists of strongly strained greenish chlorite–muscovite schists, grey metasandstones, quartz veins and concordant foliated pegmatite bodies. Shear bands, i.e., *S–C'* structures, are widespread and suggest that this is a shear zone with a top-to-the-NE sense of movement. Relics of an older foliation with discordant pegmatite dykes are locally preserved in strain shadows, outside which pegmatites are transposed to parallelism with the shear foliation. This shear zone was attributed to Paleozoic tectonism, probably Devonian, on structural grounds only (Shackleton et al., 1979). However, one foliated granite within the zone yielded

an Ordovician age of ca. 464 Ma that was argued by Loewy et al. (2003) as emplaced shortly prior to the low-grade metamorphism (M3). The large *Atico igneous complex* consists in large part of diorites variably retrogressed to chlorite – epidote – albite, and abundant pegmatite dykes. This complex, along with its southern prolongation in the Camaná igneous complex, was attributed an age of ca. 450 Ma by Shackleton et al. (1979) on the basis of a combined Rb–Sr whole-rock isochron.

### 2.2. The southern section

The *Camaná–Mollendo domain* is the largest one and consists of high-grade rocks that underwent granulite facies UHT metamorphism, with a paragenesis containing orthopyroxene + sillimanite + quartz and sapphirine + quartz (Martignole and Martelat, 2003). It consists for the most part of monotonous banded migmatitic gneisses formed by variably restitic mesosomes and alternating leucosomes (Fig. 2a). Augen–gneisses are found locally, such as near Mollendo, that probably formed by stretching of banded migmatites within strongly strained shear zones. Peneconcordant but unstrained muscovite pegmatite sheets are irregularly distributed throughout the domain, more abundant in the north and northwest between Quilca and Camaná. Foliation is very regular over long distances. However changes in dip and strike can be mapped on a regional scale due to large upright post-foliation folds. Small-scale (cm to m) syn-foliation folds are locally found.

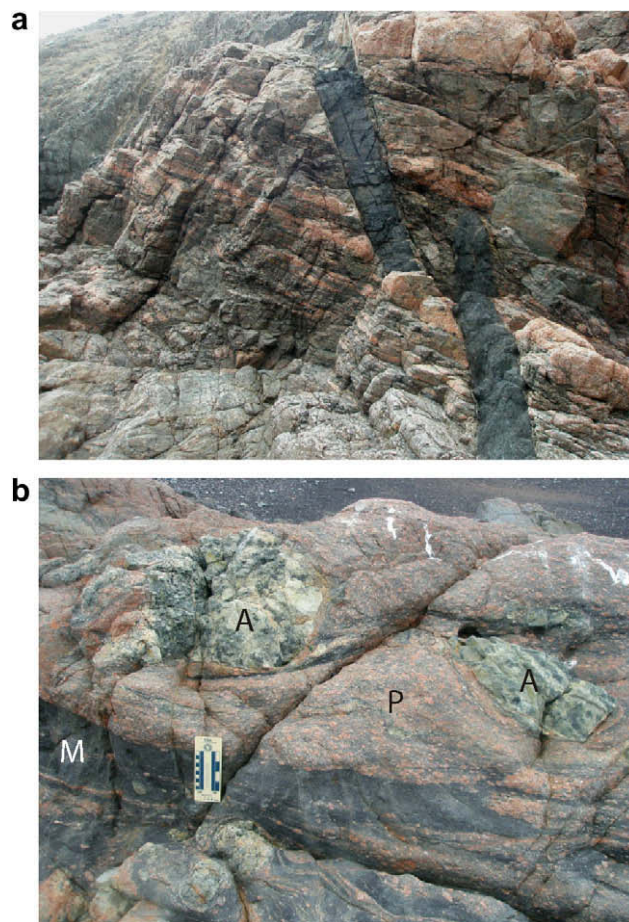


**Fig. 2.** (a) Banded migmatitic gneisses near Quilca traversed by Cainozoic basaltic dykes. (b) Basement outcrop near Ilo. Mylonitic porphyritic granites (P) with disrupted anorthosite lenses (A), and dark bands of fine-grained mylonitic gneisses (M).

### 2.3. The Ilo domain

The southernmost *Ilo domain* is separated from the main Massif by a cover of Mesozoic and Cenozoic sedimentary rocks. This domain is a medium- to low-grade shear zone with strongly retrogressed igneous protoliths. The main facies is reddish, variably foliated, porphyritic granite. Boudins of coarse anorthosite that resulted from stretching of older larger bodies are aligned within the foliated porphyritic granite. A third facies consists of narrow bands, parallel to foliation, of a dark fine-grained mylonitic rock that contains irregularly distributed feldspar porphyroclasts. Contacts are sharp or gradual. Some bands look like sheared porphyritic granites; others as appear to be derived from dykes that underwent local mingling with the host granite. Strain increases from anorthosite through the dark bands to the granite; mylonitic foliation is common (Fig. 2b). Martignole et al. (2005) considered the protoliths to be part of a Grenvillian AMCG suite.

### 3. Sampling and petrographic description

Out of a larger sampling of the whole Massif from San Juan down to Ilo, eight samples were chosen for U–Pb SHRIMP dating of zircons and eight for Nd isotope composition. Two muscovite samples were collected from pegmatites. Sampling was aimed at deciphering the complex geological history of this basement and particularly to constrain the age of the Grenvillian tectonothermal event. Because of the tectonic implications and the expected influence of the alleged Grenvillian anorthosite magmatism in UHT metamorphism (e.g., Arima and Gower, 1991, and references therein) one target was the anorthosite and allied rocks from Ilo. Determining the protoliths of many of the metamorphic rocks was difficult, particularly for the highly recrystallized rocks of the Camaná–Mollendo domain, and so five high-grade gneisses from this domain were also analysed for REE.

Sample locations are shown in Fig. 1. Coordinates, description, abbreviated mineralogy and the analytical work carried out on each sample are shown in Table 1. More detailed petrographic descriptions of the rocks can be found in Supplementary Table 1, obtainable from the Journal of South American Earth Sciences Supplementary data File #1.

### 4. Analytical methods

Samples for Sr and Nd isotope analysis were crushed and powdered to ~200 mesh. Powders were first decomposed in 4 ml HF and 2 ml HNO<sub>3</sub> in Teflon digestion bombs for 48 h at 120 °C, and finally in 6 M HCl. Elemental Rb, Sr, Sm and Nd were determined by isotope dilution using spikes enriched in <sup>87</sup>Rb, <sup>84</sup>Sr, <sup>149</sup>Sm and <sup>150</sup>Nd. Ion exchange techniques were used to separate the elements for isotopic analysis. Rb, Sr and REE were separated using Bio-Rad AG50 × 12 cation exchange resin. Sm and Nd were further separated from the REE group using bio-beads coated with 10% HDEHP. All isotopic analyses were carried out on a VG Sector 54 multicollector mass spectrometer at the Geocronología y Geoquímica Isotópica Laboratory, Complutense University, Madrid, Spain. Nd and Sr isotope data are shown in Tables 2 and 3, respectively. REEs were analysed at ACTLABS (Canada) by ICP MS (Table 4).

U–Pb analyses were performed on eight samples using SHRIMP RG at the Research School of Earth Sciences, The Australian National University, Canberra. Zircon fragments were mounted in epoxy together with chips of the Temora reference zircon, ground approximately half-way through and polished. Reflected and transmitted light photomicrographs, and cathodo-luminescence (CL) SEM images, were used to decipher the internal structures of the sectioned grains and to target specific areas within the zircons. Each analysis consisted of six scans through the mass range. The data were reduced in a manner similar to that described by Williams (1998, and references therein), using the SQUID Excel macro of Ludwig (2001). U–Pb data are in Supplementary Table 2 obtainable from the Journal of South American Earth Sciences Data File 2#. Results are shown in Figs. 3–5 and described below.

### 5. Zircon SHRIMP U–Pb samples and results

#### 5.1. MAR-8

Fine-grained gneiss (meta-igneous) (Fig. 3a). Zircons are elongate (less than 150 μm in length) sub-rounded to euhedral in shape. CL images show that most grains consist of a core and a rim. Cores are elongate euhedral prisms, although with resorption features, with oscillatory zoning that reflects an igneous origin. Rims show low-luminescence and are large enough to be analysed.

**Table 1**  
Short description of rocks selected for U–Pb SHRIMP zircon dating and geochemistry.

Sample	Coordinates	Domain	Rock type <sup>*</sup>	Abbreviated mineralogy <sup>**</sup>	Analytical work
MAR-8	15°24'21.3"S, 75°08'16.8"W	S. Juan Marcona	Fine-grained gneiss. Dacitic to rhyodacitic Low-grade retrogression: strong	Qtz, Pl, Kfs, Ms, Chl, Op, Cb, Zrn	S
OCO-26	16°26'32.5"S, 73°07'24.7"W	S. Juan Marcona	Medium-grade metasedstone	Qtz, Pl, Ms, Bt, Zrn	S
CAM-2	16°32'17.2"S, 72°31'23.2"W	Camaná–Mollendo	Banded migmatitic gneiss	Qtz, Pl, Kfs, Opx, Sil, Bt, Mag, Zrn	S, I, R
CAM-6	16°30'40.3"S, 72°38'16.6"W	Camaná–Mollendo	Gneiss (mesosome)	Qtz, Kfs, Pl, Grt, Sill, Mag, Bt, Chl, Ser, Zr, Ap, Sp	I, R
CAM-7	16°30'40.3"S, 72°38'16.6"W	Camaná–Mollendo	Banded migmatitic gneiss	Qtz, Kfs, Pl, Grt, Sil, Bt, Mag, Zrn	S, I, R
QUI-10	16°42'52.9"S, 72°25'18.9"W	Camaná–Mollendo	Banded migmatitic gneiss	Qtz, Kfs, Sill, Bt, Opx, Pl, Mag, Chl, Ser, Zrn, Ap	I, R
QUI-16	16°40'59.3"S, 72°20'05.9"W	Camaná–Mollendo	Banded migmatitic gneiss	Qtz, Pl, Kfs, Bt, Sill, Grt, Mag, Ser, Chl, Zrn	S, I, R
MOL-17	16°54'59.2"S, 72°02'50.4"W	Camaná–Mollendo	Augen-gneiss	Qtz, Kfs, Pl, Grt, Sil, Mag, Bt, Ser, Ep, Chl, Zrn	S
ILO-19	17°27'59.2"S, 71°22'19.9"W	Ilo	Reddish mylonitic porphyritic granite. Low-grade retrogression: strong	Qtz, Chl, Ep, Pl, Kfs, Ttn, Ilm, Ser, Aln, Ap, Fl, Zr	S, I, R
ILO-20	17°27'59.2"S, 71°22'19.9"W	Ilo	Mylonitic dark gneiss. Low-grade retrogression: moderate	Qtz, Pl, Hb, Bt, Chl, Ser, Ep, Aln, Mt, Ap, Zrn	S, I, R
ILO-23	17°28'56.1"S, 71°21'56.4"W	Ilo	Coarse grained anorthosite. Low-grade retrogression: minor	Pl, Hb, Bt, Ttn, Rt, Ilm, Ser, Chl, Ep	S, I, R

Analytical work: S = U–Pb SHRIMP; I = Nd isotope composition; R = REEs chemical analysis.

<sup>\*</sup> For a detailed description see Supplementary Table in Data Repository.

<sup>\*\*</sup> Mineral abbreviations according to Siivola and Schmid (2007). Order reflects relative modal amounts.

**Table 2**  
Sm–Nd isotope composition of selected rocks from the Camaná–Mollendo and Ilo domains.

Sample	Sm (ppm)	Nd (ppm)	Sm/Nd	$^{147}\text{Sm}/^{144}\text{Nd}$	$^{143}\text{Nd}/^{144}\text{Nd}$	$\epsilon\text{Nd}_{465}$	$T_{\text{DM}}(465)$	$\epsilon\text{Nd}_{1000}$	$\epsilon\text{Nd}_{1700}$	$T_{\text{DM}}$
CAM-2	5.59	30.3	0.1845	0.1115	0.511333			–14.6	–6.9	2445
CAM-6	6.57	34.4	0.1910	0.1154	0.511348			–14.8	–7.5	2513
CAM-7	5.1	27.1	0.1882	0.1137	0.511294			–15.6	–8.2	2549
QUI-10	7.3	39.9	0.1830	0.1106	0.511322			–14.7	–6.9	2440
QUI-16	6.57	37.5	0.1752	0.1059	0.511343			–13.7	–5.5	2314
ILO-19	8.01	50.7	0.1580	0.0955	0.511996	–6.4	1691			
ILO-20	10	60	0.1667	0.1007	0.511940	–7.8	1791			
ILO-23	1.02	4.46	0.2287	0.1383	0.512274	–3.6	1483			

Nd isotopic ratios were normalized to  $^{146}\text{Nd}/^{144}\text{Nd} = 0.7219$ .  
 La Jolla Nd standard gave a mean  $^{143}\text{Nd}/^{144}\text{Nd}$  of  $0.511847 \pm 0.00001$  ( $n = 9$ ).  
 The  $2\sigma$  analytical errors are 0.1% in  $^{147}\text{Sm}/^{144}\text{Nd}$  and 0.006% in  $^{143}\text{Nd}/^{144}\text{Nd}$ .  
 Decay constant was  $\lambda_{\text{Sm}} = 6.54 \times 10^{-12} \text{ a}^{-1}$ .  
 $T_{\text{DM}}$  is model age according to DePaolo et al. (1991).  
 $^{147}\text{Sm}/^{144}\text{Nd}$  and  $^{143}\text{Nd}/^{144}\text{Nd}$  values assumed to be 0.1967 and 0.512636 for CHUR, and 0.222 and 0.513114 for depleted-mantle, respectively.

**Table 3**  
Rb–Sr composition of muscovite from pegmatites.

Sample	Rb	Sr	Rb/Sr	$^{87}\text{Rb}/^{86}\text{Sr}$	$^{87}\text{Sr}/^{86}\text{Sr}$	Model age Ma
JC-01C Ms	609.412	6.52	93.4681	463.637	8.011008	1100
QUI-005 Ms	526.469	6.664	79.0020	338.286	5.614221	1015

Sr isotopic ratios were normalized to  $^{86}\text{Sr}/^{88}\text{Sr} = 0.1194$ .  
 NBS987 standard gave a mean  $^{87}\text{Sr}/^{86}\text{Sr}$  ratio of  $0.710216 \pm 0.00005$  ( $n = 10$ ).  
 The  $2\sigma$  analytical errors are 1% in  $^{87}\text{Rb}/^{86}\text{Sr}$ , 0.01% in  $^{87}\text{Sr}/^{86}\text{Sr}$ .  
 Decay constants used were  $\lambda_{\text{Rb}} = 1.42 \times 10^{-11} \text{ a}^{-1}$ .  
 Model ages assumes initial  $^{87}\text{Sr}/^{86}\text{Sr}$  values between 0.703 and 0.715

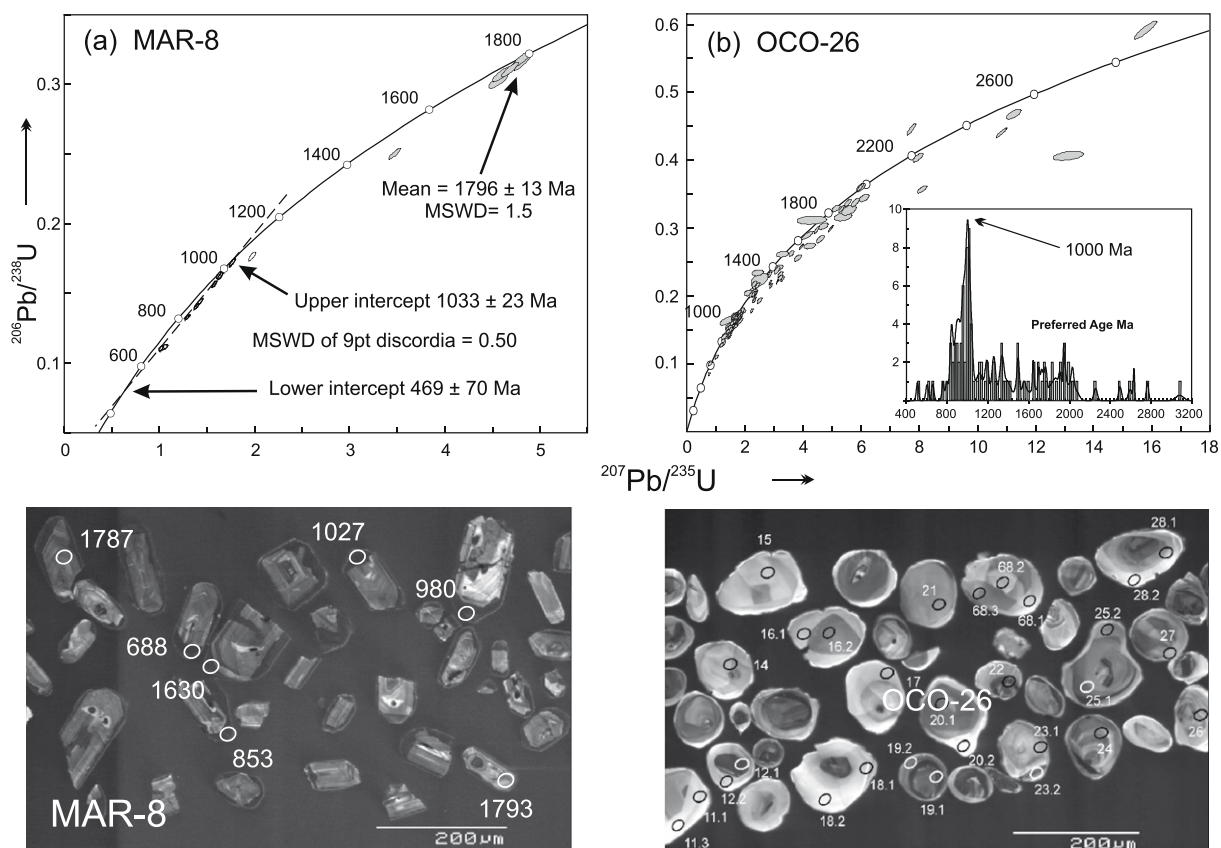


**Fig. 3.** U–Pb SHRIMP data for samples from the northern section of the Arequipa Massif.  $^{204}\text{Pb}$ -corrected data are plotted as  $1\sigma$  error ellipses in Wetherill Concordia diagrams, with typical cathodo-luminescence images displayed below. (a) MAR-8 (San Juan Marcona) shows data for cores (grey shading) trending away from ca. 1800 Ma, interpreted as an igneous protolith age, and rims (white ellipses) plotting on a Discordia between ca. 1000 Ma (Grenvillian age of main metamorphism) towards ca. 470 Ma (Famatinian overprint). (b) OCO-26 (Atico) shows a rather discordant spread of data from Archaean to Neoproterozoic, with the  $^{207}\text{Pb}/^{206}\text{Pb}$  ages concentrating at ca. 1000 Ma (metamorphism).

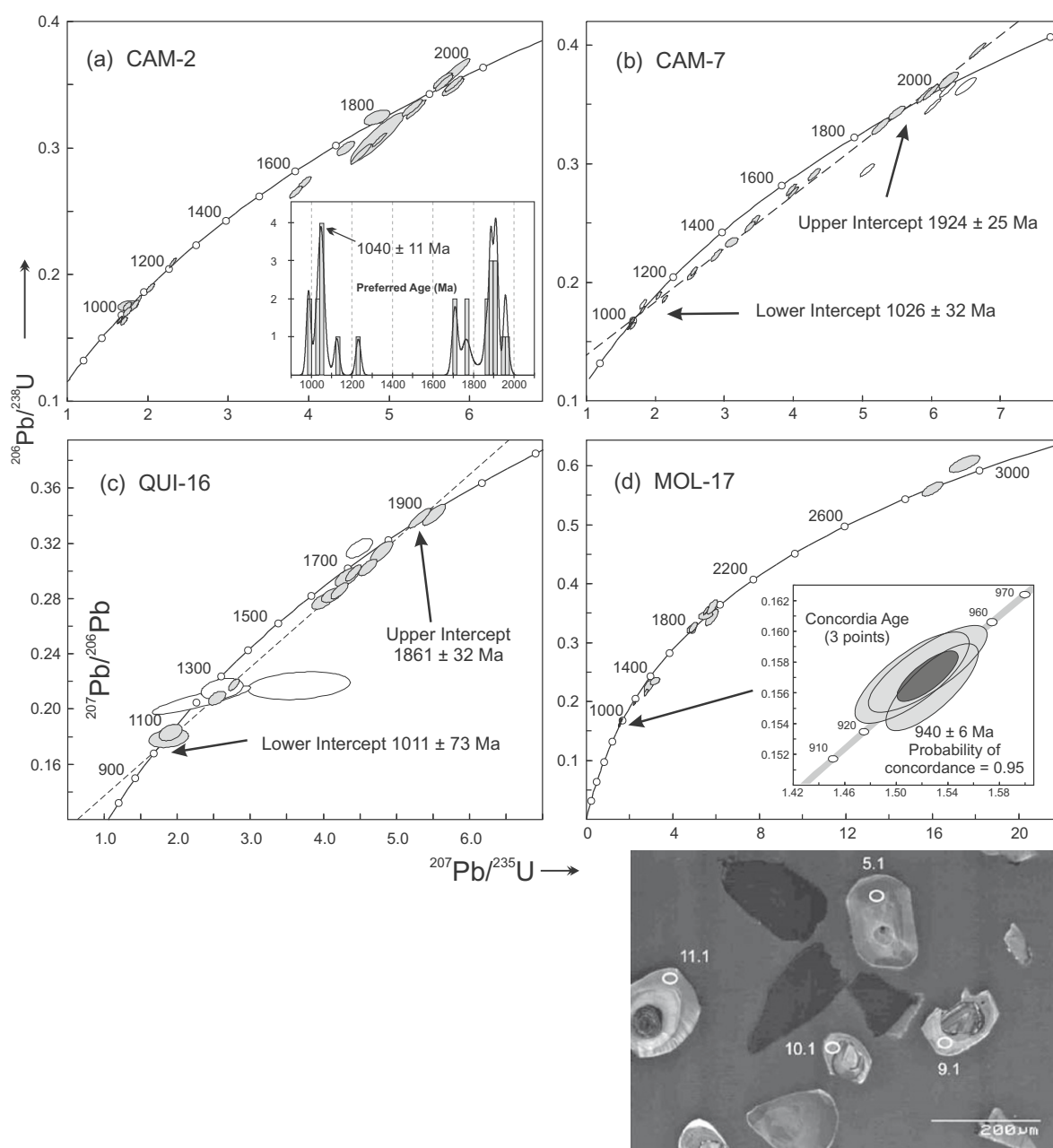


**Fig. 4.** U–Pb SHRIMP data for samples from the southern section of the Arequipa Massif.  $^{204}\text{Pb}$ -corrected data are plotted as  $1\sigma$  error ellipses in Wetherill Concordia diagrams. (a) CAM-2 shows a strong bipolar distribution of ages ( $^{206}\text{Pb}/^{238}\text{U}$  for  $<1000$  Ma,  $^{207}\text{Pb}/^{206}\text{Pb}$  for  $>1000$  Ma), indicating Pb-loss from a major event at ca. 1900 Ma and a second concentration around 1000 Ma. (b) CAM-7 and (c) QUI-16 show similar patterns with additional discordance (white ellipses indicate data ignored in the discordia fit). (d) MOL-17 from the Mollendo area (cathodo-luminescence image shown below) also has three highly concordant data points for zircon rims at 940 Ma.

Eighteen points were analysed including rims and cores. Nine cores yielded  $^{207}\text{Pb}/^{206}\text{Pb}$  ages between 1210 and 1813 Ma. If analyses with discordance  $>10\%$  are rejected (#12 and #17), the remaining spots plot near Concordia and yield a mean  $^{207}\text{Pb}/^{206}\text{Pb}$  age of  $1796 \pm 13$  Ma (MSWD = 1.5), which is interpreted as the crystallization age of the igneous protolith. The high Th/U values of cores (0.32–0.34), typical of igneous zircons, reinforce this interpretation. Rims are high-U (mostly over 1000 ppm) and with very low Th/U values (mostly  $<0.2$ ) typical of a metamorphic origin. Rim analyses plot on a discordia with an upper intercept at  $1033 \pm 23$  Ma and a lower intercept at  $469 \pm 70$  Ma; taken as the ages of Grenvillian metamorphism and Early Paleozoic overprint, respectively. The latter gave rise to more pronounced Pb-loss in the Grenvillian rims than in the relict cores.

## 5.2. OCO-26

Metasandstone (Fig. 3b). The zircons from this sample are mostly equant, round to sub-round grains that range up to 200  $\mu\text{m}$  in diameter but with many less than 50–100  $\mu\text{m}$ . The grains are generally clear and colourless, with only some clouded grains, and some that may be frosted due to surface transport. The CL images reveal a complex internal structure (Fig. 3b). Many grains comprise a zoned igneous centre, overgrown by metamorphic zircon with homogeneous CL. Also common are grains with metamorphic central areas with lighter or darker CL outermost metamorphic zircon. Some grains have multiple stages of zircon growth, the outermost invariably being a bright CL metamorphic rim.

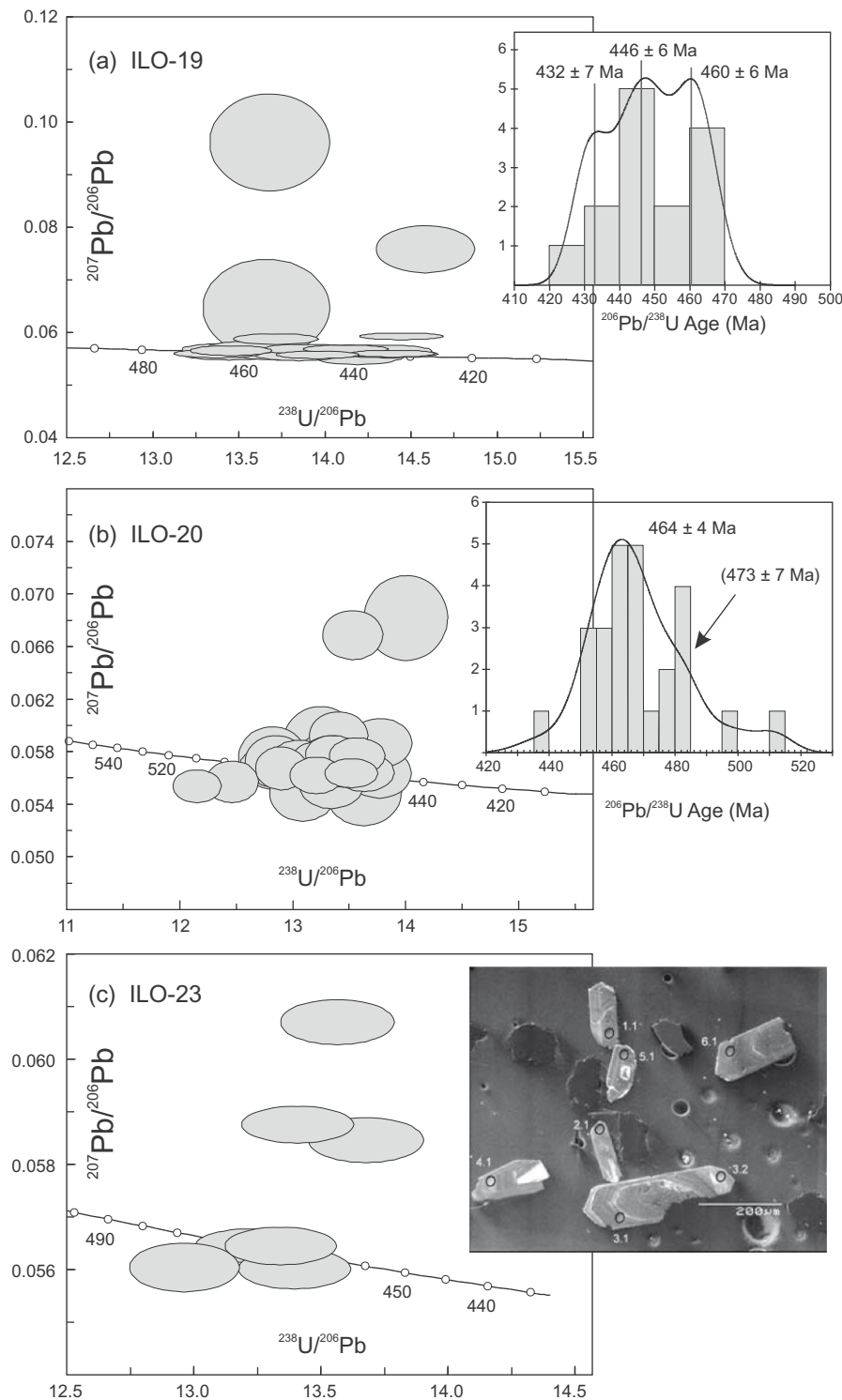


**Fig. 5.** U–Pb SHRIMP data for samples from the Ilo domain. Uncorrected data are plotted as  $1\sigma$  error ellipses in Tera–Wasserburg diagrams. All data plot with Ordovician extrapolated ages, but with a significant spread along Concordia. For (a) ILO-19 and (b) ILO-20, the insets show attempts at unmixing the ages. For (c) ILO-23 (anorthosite) insufficient data were obtainable for detailed treatment, but the cathodo-luminescence image inset shows good igneous concentric zoning to support interpretation of the magmatic crystallization as Ordovician in age.

Given the complex nature of the zircon population, 105 areas were analysed on 70 zircon grains. The analyses range up to 30% discordant, although many are within analytical uncertainty of Concordia in both the Wetherill ( $^{204}\text{Pb}$ -corrected data) and Tera–Wasserburg (data uncorrected for common Pb) diagrams. The relative probability plot shows a major peak at 1000 Ma, with slightly

younger subordinate groups of analyses at ca. 940 Ma and ca. 840 Ma, a sequence of minor peaks through the Mesoproterozoic (ca. 1200, 1260, 1340, 1500), and a significant concentration in the interval 1650–2030 Ma, as well as a few older ages back to 2770 Ma (Archaean). The older ages are comparable to those seen in other samples reported here. We interpret the major peak at ca.



**Table 4**  
REE analyses of granulites.

	CAM-2	CAM-6	CAM-7	QUI-10	QUI-16
La	42.8	46.4	37.7	58.1	55.3
Ce	86.1	93.2	76.8	115	110
Pr	9.46	10.5	8.43	12.4	11.8
Nd	30.3	34.4	27.1	39.9	37.5
Sm	5.59	6.57	5.1	7.3	6.57
Eu	1.32	1.28	1.1	1.71	1.5
Gd	4.44	5.54	3.94	5.32	4.88
Tb	0.75	0.89	0.63	0.86	0.76
Dy	4.44	5.09	3.56	4.93	4.21
Ho	0.88	0.96	0.68	0.92	0.77
Er	2.49	2.72	1.84	2.55	2.1
Tm	0.36	0.39	0.26	0.34	0.28
Yb	2.28	2.42	1.57	2.15	1.62
Lu	0.33	0.35	0.23	0.33	0.24
REE	191.5	210.7	168.9	251.8	237.5
(La/Yb) <sub>N</sub>	13.5	13.8	17.2	19.4	24.5
(La/Sm) <sub>N</sub>	4.9	4.6	4.8	5.1	5.4
(Gd/Yb) <sub>N</sub>	1.6	1.9	2.1	2.0	2.5
Eu/Eu*	0.8	0.6	0.8	0.8	0.8

1000 Ma as corresponding to peak metamorphism of Grenville-age in the Atico domain. All older ages are interpreted as reflecting detrital grains, mostly igneous, but also metamorphic mantles.

The data giving the youngest ages tend to plot above the Concordia curve in the Tera-Wasserburg diagram (not shown), in part forming a Pb-loss discordia. These areas are considered to have lost radiogenic Pb and are not interpreted as reflecting Neoproterozoic metamorphic zircon. However, the presence of ages of 850–950 Ma in the analyses of the outer areas and rims to structured grains record mean that a case can be made for metamorphic zircon development later than 1000 Ma.

On the basis of this interpretation, peak metamorphism occurred at *ca.* 1000 Ma and the sedimentary protolith may well have formed between this time and the next oldest minor peak at *ca.* 1200 Ma, i.e., Late-Mesoproterozoic.

### 5.3. CAM-2

Migmatitic gneiss (mesosome) (Fig. 4a). The zircons from this sample are equant-to-elongate, round to sub-round in shape and less than 200  $\mu\text{m}$  in length. The CL images reveal a range of internal structures. Some areas are zoned igneous zircon, whilst other areas have an irregular wispy structure, and yet others areas are broad and homogeneous. These features indicate a range of zircon crystallization events from simple igneous crystallization, to recrystallized zones and then finally metamorphic zircon growth.

Twenty-four areas were analysed on 21 zircon grains covering the range of internal CL structures, and yielding a bimodal distribution. In general the zoned igneous zircon yields older Proterozoic dates, whereas the more homogeneous metamorphic areas yield Grenvillian dates. But this is not always the case: the outer more homogeneous areas on grains #16 and #18 both yield older Proterozoic dates, whilst the weakly zoned area analysed on grain #17 is Grenvillian in age. Centres and rims were analysed on grains #10, #15 and #21. Both areas on grain #10 yield concordant Grenville dates, though the irregularly zoned core (#10.2) is older than the homogeneous metamorphic rim (#10.1). The irregularly zoned core of grain #15 is *ca.* 1960 Ma whereas the homogeneous rim is *ca.* 1050 Ma. The zoned core of grain #21 is *ca.* 1890 Ma, with the homogeneous rim Grenvillian at *ca.* 1040 Ma.

Overall, the older group consists of igneous and perhaps metamorphic core zircon with a range of nearly concordant  $^{207}\text{Pb}/^{206}\text{Pb}$  ages of 1760–1950 Ma, but with a composite peak at *ca.* 1900 Ma. The Grenvillian metamorphic group is rather variable with, at the older end, one concordant age at 1125 Ma and one less so at *ca.*

1210 Ma, and at the younger end, two  $^{206}\text{Pb}/^{238}\text{U}$  ages less than 1000 Ma that probably indicate either Pb-loss of Grenvillian areas or a superimposed thermal event peaking at *ca.* 980 Ma. The weighted average of the six remaining  $^{206}\text{Pb}/^{238}\text{Pb}$  ages is  $1040 \pm 11$  (MSWD = 0.90), which is taken as the peak of Grenvillian metamorphism.

### 5.4. CAM-7

Migmatitic gneiss (mesosome) (Fig. 4b). The zircons from this sample are round, equant-to-elongate grains that range from less than 100  $\mu\text{m}$  in diameter to 200  $\mu\text{m}$  or more in length. A few multi-lobate grains are present, representing metamorphic overgrowths. The CL images, as of sample CAM-2 show a variety of textures and features. There are areas of zoned igneous zircon, usually more centrally located within the grains, with both irregular and homogenous CL structures in outer areas (mantles) and rims.

Twenty-seven areas have been analysed on 20 zircon grains with rim-and-core pairs analysed for seven grains. The zoned igneous core to grain #17 has an Archaean  $^{207}\text{Pb}/^{206}\text{Pb}$  age of  $\sim 2690$  Ma whereas the more homogeneous rim area, interpreted as metamorphic, is Grenvillian in age with a  $^{206}\text{Pb}/^{238}\text{U}$  date of  $\sim 1120$  Ma. The outer areas and zoned igneous zircons provide a range of nearly concordant  $^{207}\text{Pb}/^{206}\text{Pb}$  dates, mostly around 1860–2080 Ma. The Wetherill plot for the  $^{204}\text{Pb}$ -corrected data clearly shows that whilst some areas are near Concordia at about either 1950 Ma or 1000 Ma, many of the areas analysed are discordant and would lie on a simple discordia between these two end-members. A discordia line fitted to a selected group of 22 analyses gives an upper intercept of  $1924 \pm 25$  Ma and lower intercept of  $1026 \pm 32$  Ma (MSWD = 3.7), the latter being taken as the age of peak Grenvillian metamorphism. The analyses not included in this general discordia line are for #15.2, with the youngest  $^{207}\text{Pb}/^{206}\text{Pb}$  date, and those with  $^{207}\text{Pb}/^{206}\text{Pb}$  dates older than 2000 Ma.

From the current data set it is clear that detrital igneous zircon and probably overgrowths of Paleoproterozoic age are common in this sample. New zircon formed during a Grenville-age event is present. A number of the grains/areas analysed show variable radiogenic Pb-loss at this time and so lie on a discordia trend.

### 5.5. QUI-16

Migmatitic gneiss (mesosome) (Fig. 4c). Separated zircons are mostly *ca.* 200  $\mu\text{m}$  in length, equant to slightly elongated, and sub-round in form. CL images show complex internal structures, with small relict cores (in some cases with igneous zoning) surrounded by mantles of variable thickness most of which show broad faint oscillatory zoning, and low-luminescence rims. The latter are usually complete and discordant to the earlier structures; they are of irregular thickness, up to 50  $\mu\text{m}$  or more on some grain tips. The textures are interpreted as due to detrital igneous crystals and successive stages, probably two, of metamorphic overgrowth.

Sixteen areas were analysed on 15 grains. Both core and mantle were analysed in grain #1. Two analyses (#4 and #8) were carried out on well-developed rims; their  $^{207}\text{Pb}/^{206}\text{Pb}$  ages are 1079 Ma and 1995 Ma. The other spots were on mantles: Th/U ratios are generally high (0.07–3.33, with 12 of 16 ratios being  $>0.2$ ). If the more imprecise analyses are excluded, the rest plot on a simple discordia (MSWD = 0.9) with an upper intercept at  $1861 \pm 32$  Ma and a poorly defined lower intercept at  $1011 \pm 73$  Ma.

### 5.6. MOL-17

Augen-gneiss (uncertain protolith) (Fig. 4d). The zircons from this sample are round to sub-round grains that are generally clear. The CL images show complex internal structure; many grains have

zoned igneous cores, interpreted as igneous, overgrown by more homogeneous, probably metamorphic zircon.

Sixteen grains were analysed, with most of the analyses on the more homogeneous outer areas of the grains interpreted as metamorphic. The exceptions are the analyses of grain #16, where the zoned core was also analysed (both core and rim giving Archaean ages of ca. 2900 Ma). The analyses are generally low in U and the Th/U ratios range to very high values (0.16–4.06), apart from those of grains #10 and #11 (0.08). The analyses mostly plot on a simple discordia between  $1892 \pm 62$  Ma and  $973 \pm 82$  Ma (MSWD rather high at 2.4). There are a number of discordant analyses, but these do not indicate the presence of intermediate Mesoproterozoic zircon. The three youngest Grenvillian areas are highly concordant and yield a defined Concordia age of  $940 \pm 6$  Ma (MSWD = 0.004), which is taken as the best age for the Pb-loss and possible metamorphic event. There is a possibility that this rock underwent an older thermal event responsible for the Paleoproterozoic ages of some overgrowths. The ultimate age of the protolith is unknown as insufficient data were obtained from cores.

### 5.7. ILO-19

Mylonitic porphyritic granite (Fig. 5a). The abundant zircons in this sample are elongate, mostly  $\sim 200$   $\mu\text{m}$  in length, or longer, with either sub-round or pyramidal terminations. Many grains can be seen to be strongly zoned under transmitted light and although many are clear and colourless a few are dark and metamict. CL shows a variety of internal structures. Many grains and areas within grains are simple oscillatory zoned zircon, but there are prominent grains with very irregular internal features and in places these wispy features overprint and cross-cut what is interpreted to be the primary simple igneous zoning.

Twenty-three areas were analysed on 20 grains covering the full range of complex internal CL structures. All 23 analyses yield  $^{206}\text{Pb}/^{238}\text{U}$  ages in the range 415–465 Ma and the relative probability plot shows a broad peak or peaks centred at about 450 Ma. Apart from three analyses (#3, #4.1 and #15) the data are low in common Pb and the  $^{204}\text{Pb}$ -corrected data are within uncertainty of Concordia. There is no evidence for any Grenville-age event in these zircon grains. There is a wide range in U and Th contents, but the Th/U ratios are moderate to high, reflecting the dominantly igneous nature of the zoned zircon. If the three analyses with high common Pb and all others with >10% discordance are excluded, three possible age peaks can be recognized: ca. 460 Ma, ca. 446 Ma and ca. 432. The younger peak could be related to retrogression within the shear zone (overprinting features in zircon grains) which is strong in this rock.

### 5.8. ILO-20

Dark mylonitic gneiss (Fig. 5b). The zircons from this sample are mostly slender, elongate grains with subhedral terminations. More equant and bulkier elongate grains are also present, tending to be coarser-grained, up to 250  $\mu\text{m}$  in length and 50  $\mu\text{m}$  in width. The CL images show a complex internal structure. Whilst many grains have length-parallel zoning (interpreted as igneous), more homogeneous, possibly metamorphic, zircon is present both as rims and in places forming anastomosing embayments into the zoned igneous zircon.

Twenty-six areas were analysed on 21 grains (Fig. 5b). A wide range of the internal structures noted above were analysed, with both the zoned igneous and the more homogeneous areas interpreted as metamorphic analysed on a number of single grains. The resulting data form a dispersed grouping that is dominantly within uncertainty of the Tera-Wasserburg Concordia. Two analyses, #2.2 and #6.1, are more enriched in common Pb; the former

yields a young  $^{206}\text{Pb}/^{238}\text{U}$  date of ca. 438 Ma and the area analysed is considered to have lost radiogenic Pb. The relative probability plot of  $^{206}\text{Pb}/^{238}\text{U}$  ages shows a dominant bell-shaped peak, which yields a weighted mean age of  $464 \pm 4$  (MSWD = 1.07). It is noteworthy that this grouping includes both zoned igneous and the more homogeneous zircon areas; thus the igneous emplacement and subsequent metamorphic developments in these grains occurred within the analytical uncertainty of 464 Ma. On the older age side, there is a subordinate grouping around ca. 480 Ma (four analyses give a mean of  $483 \pm 7$  Ma) and scattered older dates to ca. 512 Ma. The central areas to a number of grains were analysed as it was originally presumed that this rock would yield a Grenvillian age. However, whilst there are scattered analyses older than the dominant Ordovician peak, there is no evidence for such a Grenville event.

### 5.9. ILO-23

Anorthosite (Fig. 5c). Only a few zircon grains were separated from this sample (seven on the probe mount). They are elongate and range from clear subhedral forms to dark, metamict subhedral grains. The CL images are very dark, but relict igneous zoning can be seen.

Seven areas were analysed on six grains; they have high-U ranging from 1700 to 3065 ppm, with relatively moderate Th and Th/U ratios in the range 0.08–0.21. This is on the slightly low side for normal igneous zircon but may reflect late-stage magmatic crystallisation or partial melting. The areas analysed are low in common Pb, but not ideal in terms of zircon clarity or good CL structure. The relative probability plot for the limited number of analyses is irregular, with one clearly older analysis and some skew to the young age side. A weighted mean of the  $^{206}\text{Pb}/^{238}\text{U}$  ages for five of the seven analyses provides an estimated crystallisation date of  $464 \pm 5$  Ma (MSWD = 1.0).

## 6. Pegmatites

Because Rb is strongly fractionated in muscovite relative to Sr, the  $^{87}\text{Sr}/^{86}\text{Sr}$  ratio in the mineral increases very quickly with time and the calculated age is insensitive to the assumed initial values for calc-alkaline magmas. The ages of two muscovite samples obtained in this way were 1000 and 1100 Ma (Table 3), i.e., Grenvillian. These pegmatites, although roughly concordant to their host rocks, do not show evidence for ductile deformation and/or superimposed metamorphism, and the Rb–Sr ages are taken as approximately dating magmatic crystallization.

## 7. REE and Nd isotope data

REE data for five samples of high-grade gneisses from the Camaná–Mollendo domain (Table 4) are plotted in Fig. 6. They show enrichment in LREE relative to HREE, with  $(\text{La}/\text{Yb})_N$  values between 13.5 and 24, and a small negative Eu anomaly ( $\text{Eu}/\text{Eu}^* = \text{ca. } 0.8$ ). REE patterns are remarkably similar in the five gneisses suggesting that they were all derived from the same type of protolith. They are also strikingly similar to those of shales, e.g., the North American Shale Composite (Taylor and McLennan, 1988), so that it may be inferred that the gneisses were derived from detrital sedimentary rocks. The small differences among the five rocks analysed here may be attributed to variable melt extraction during migmatization.

Nd isotope composition is available for the five high-grade gneisses (Table 2). They yielded  $\epsilon\text{Nd}_t$  values of  $-5.5$  to  $-8.2$  at the reference age of 1700 Ma. Nd single-stage depleted-mantle model ages ( $T_{\text{DM}}$ , DePaolo, 1981) range between ca. 2.3 and 2.5 Ga.

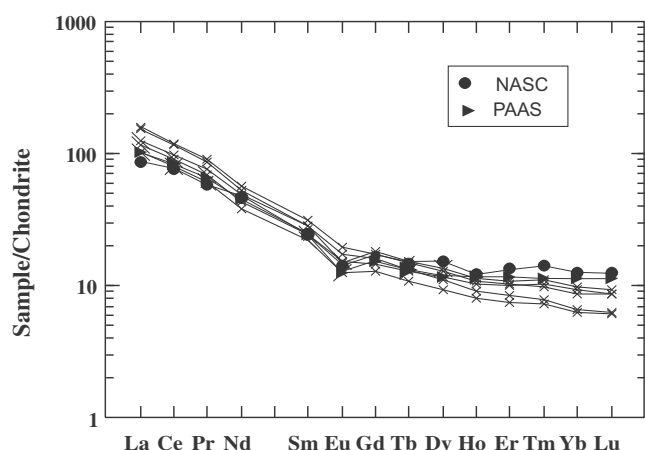


Fig. 6. Chondrite-normalized REE patterns of migmatitic gneisses. The North America Shale Composite REE pattern (Taylor and McLennan, 1988) is added for comparison.

Nd isotope composition is also available for three meta-igneous rocks from the Ilo domain.  $\epsilon_{\text{Ndt}}$  values at the reference age of 475 Ma (Table 2) differ significantly from one rock to another:  $-6.4$  (ILO-19),  $-7.8$  (ILO-20) and  $-3.6$  (ILO-23), the latter being for the anorthosite. The value for ILO-20, the mafic gneiss, is less primitive than that of the granite, perhaps indicating different protoliths and not only strain differences between the two rocks as might be argued from field evidence alone.

## 8. Discussion

Two views emerge from these data: (1) the geological history of the Arequipa Massif covers a very long period of time, between Paleoproterozoic and Early Paleozoic (Ordovician/Silurian), and (2) three main rock-forming events took place, at widely separated times: in the Paleoproterozoic, in the Late-Mesoproterozoic and in the Paleozoic.

### 8.1. The Paleoproterozoic. An old orogenic history

The protolith of the strongly retrogressed quartzose gneiss MAR-8 from the San Juan Marcona domain was a felsic igneous rock, probably volcanic or subvolcanic. Its age of  $1796 \pm 13$  Ma (Late Paleoproterozoic) coincides with a discordia upper intercept age of  $1793 \pm 6$  Ma found by Loewy et al. (2004) for a retrogressed foliated megacrystic granite nearby (sample U/Pb-3). The age of ca. 1.79 Ga thus corresponds to an event of felsic magmatism. Moreover, this age constrains the age of the host metasedimentary rocks that were coeval or older.

Migmatitic gneisses of the Camaná–Mollendo domain, although separated from the San Juan domain by the Atico medium-grade rocks and the Ocoña phyllonite zone, probably correspond to the same geological domain, although they are generally less retrogressed and appear to contain material older than the igneous protolith in the San Juan Marcona domain. Most of the migmatitic gneisses are probably metasedimentary, as inferred from both the similarity of their REE pattern to those of shales and the high peraluminosity evidenced by the mineral compositions (Martignole and Martelat, 2003).

All the samples contain Paleoproterozoic zircons that underwent a metamorphic overprint of Grenvillian age. Low-discordance Paleoproterozoic ages range from 1.76 to 2.1 Ga. A few scattered Archaean zircons were also found (ca. 2.7 Ga in CAM-7, ca. 2.9 Ga in MOL-17). Moreover, the Paleoproterozoic ages embrace detrital

cores with relict igneous zoning and thick sub-rounded, homogeneous or weakly concentrically-zoned, overgrowths (mantles). The latter features are common in high-grade metamorphic zircons (Vavra et al., 1999; Corfu et al., 2003). Most of the analysed areas were overgrowths, most of them with Th/U values higher than most metamorphic zircons (which tend to have values  $<0.1$ ). This fact however has been also recognized in other high-grade metamorphic areas (e.g., Goodge et al., 2001) and, of particular relevance, in UHT metamorphic regions, e.g., in the Napier Complex, Antarctica (Carson et al., 2002). Such high Th/U values in metamorphic mantles are attributed to U-depletion during UHT metamorphism prior to zircon growth (Black et al., 1986; Carson et al., 2002). We propose that the zircon overgrowths in the Arequipa Massif migmatitic gneisses probably resulted from UHT metamorphism during the Paleoproterozoic.

Samples CAM-2 and CAM-7 contain detrital igneous cores of 1890–2080 Ma that along with the few Archaean cores referred to above, suggest magmatic events in the source area of the sedimentary protoliths in the Middle Paleoproterozoic (Rhyacian and Orosirian) and in the Archaean. Most of the analysed zircon areas plot on discordias resulting from Pb-loss during Grenvillian metamorphism, and as most correspond to mantles on older cores, the upper intercept ages probably date metamorphism. The strongest cases are for samples QUI-16 and MOL-17, where only overgrowths were considered for regression; the resulting ages are  $1861 \pm 32$  Ma and  $1892 \pm 62$  Ma, respectively. Thus a metamorphic event at ca. 1.87 Ga is inferred for the Paleoproterozoic overgrowths. Whether these Paleoproterozoic overgrowths formed *in situ* or were detrital is more difficult to assess. Zircon grains in samples QUI-16 and MOL-17 show overgrowths that are quite regular and complete around detrital igneous cores (Fig. 4). This might be taken as compatible with overgrowth formation *in situ* and consequently with a metamorphic event in the Camaná–Mollendo domain at ca. 1.87 Ga. This interpretation strengthens that of Loewy et al. (2004), who argued on geological grounds for a metamorphic event (M1) and deformation at ca. 1.8 Ga, i.e., prior to the intrusion of the megacrystic granite (U/Pb3). Consequently, the age of the sedimentary protoliths of the migmatitic gneisses can now be bracketed with some confidence between ca. 1.87 and the minimum age of detrital igneous zircons, i.e., ca. 1.9 Ga. In consequence sedimentary protoliths formed shortly before metamorphism. Quite similarly Cobbing et al. (1977), Dalmayrac et al. (1977) and Shackleton et al. (1979) argued in favour of a granulite facies regional metamorphism between ca. 1.8 and 1.95 Ga, with protolith ages of ca. 2000 Ma. However, these authors considered that the granulitic gneisses resulted from a single metamorphic event and did not recognize the superimposed Grenvillian event (see below).

Nd isotope values ( $T_{\text{DM}}$  between ca. 2.3 and 2.55 Ga) suggest that Nd in the Camaná–Mollendo migmatitic gneisses is largely reworked from an old continental crustal material, Paleoproterozoic and/or Archaean. This is compatible with the presence in some samples of old detrital zircons of ca. 2690 Ma (CAM-7) and ca. 2900 Ma (MOL-17) that indicate an Archaean source. Moreover, the crustal source of the zircons experienced magmatism at different times between ca. 1.9 and 2.1 Ga, probably with addition of a juvenile component to the upper continental crust. This constitutes a significant fingerprint of the source area, i.e., old Nd model ages and a younger zircon population.

As for the Paleoproterozoic, the pattern that emerges from zircon ages and the geological and geochemical evidence is one of an orogeny between ca. 1.79 and 2.1 Ga (Orosirian to Rhyacian) involving: (a) early magmatism (between 1.89 and 2.1 Ga), presumably through partly Archaean continental crust, (b) sedimentation of a thick sequence of terrigenous sediments, (c) UHT metamorphism at ca. 1.87 Ga, and (d) late felsic magmatism at ca. 1.79 Ga.

### 8.2. The Atico domain: a Mesoproterozoic sedimentary basin

The only sample from this medium-grade metamorphic domain (OCO-26) shows similarities to the migmatitic gneisses of the Camaná–Mollendo domain, but also significant differences. Many low-discordance areas yield ages between 1700 and 2030 Ma and a few are Archaean, between 2600 and 2800 Ma (one discordant age *ca.* 3100 Ma). These ages are from detrital igneous cores and metamorphic mantles, and are similar to the Proterozoic to Archaean low-discordance ages found in the Camaná–Mollendo and San Juan domains. On the other hand, OCO-26 contains zircons with nearly concordant ages between *ca.* 1200 and *ca.* 1600 Ma. This group of ages has not been recognized in the high-grade domains; we interpret these zircons as detrital. Grenvillian metamorphism started at *ca.* 1000 Ma.

Deposition of the sedimentary protolith of OCO-26 occurred between *ca.* 1200 and *ca.* 1000 Ma, i.e., in the Late-Mesoproterozoic. Detrital zircons were fed from a source area similar to the high-grade Camaná–Mollendo and San Juan domains, but also from an unknown source that provided the Mesoproterozoic zircons of 1200–1600 Ma. The Atico domain can thus be interpreted as a sedimentary basin deposited on a Paleoproterozoic high-grade basement consisting of igneous and metamorphic rocks. Cobbing et al. (1977) first considered the Atico metasedimentary rocks to be younger than the Mollendo high-grade gneisses because of the presence of quartzites, absent in Camaná–Mollendo domain. However this opinion was challenged by Wasteneys et al. (1995).

### 8.3. The Grenville-age metamorphic event

All the zircon populations from the San Juan, Atico and Camaná–Mollendo samples show the imprint of a metamorphic event Late-Mesoproterozoic to Early Neoproterozoic in age. This metamorphism produced Pb-loss on both older zircon igneous cores and on Paleoproterozoic overgrowths, giving rise to linear discordias, and probably new overgrowths in the form of contrasting luminescence rims. Recorded Grenvillian ages can be bracketed between *ca.* 940 and *ca.* 1080 Ma, taking age uncertainties into account. In the Camaná–Mollendo domain Grenvillian ages are apparently older in the Quilca and Camaná samples (CAM-2:  $1040 \pm 11$  Ma; CAM-7:  $1026 \pm 32$  Ma; QUI-16:  $1011 \pm 73$  Ma) than in the Mollendo sample (MOL-17:  $940 \pm 6$  Ma), a fact that was also recognized by Wasteneys et al. (1995; point C:  $966 \pm 5$  Ma) and by Loewy et al. (2004; sample U/Pb-2:  $935 \pm 14$  Ma). Sample MAR-8 from the San Juan Marcona domain yielded an age of  $1033 \pm 23$  Ma for the Grenvillian event, i.e., within error of those of the southern Camaná–Mollendo domain. The weighted average age of metamorphism in Northern Camaná–Mollendo and San Juan Marcona is  $1037 \pm 19$  Ma. In the Atico domain we found a spread of Grenvillian ages between *ca.* 1000 and *ca.* 840 Ma. The latter domain underwent only Grenvillian metamorphism, in contrast with the Camaná–Mollendo domain, which besides Grenvillian metamorphism underwent an older Paleoproterozoic event. Martignole and Martelat (2003) carried out chemical dating of monazites from the Camaná–Mollendo domain and found a spread of Grenvillian ages; statistically meaningful ages of *ca.* 1000 Ma were obtained for three samples near Camaná. Moreover, muscovite pegmatites, probably migmatitic melts, were emplaced during the Grenvillian event (1000 and 1100 Ma) as inferred from the Sr isotope composition of muscovites presented here.

Grenville-age metamorphism at Arequipa took thus place in as many as three separate episodes: (1) *ca.* 1040 Ma in the Quilca and Camaná areas of the Camaná–Mollendo domain, and in the San Juan Marcona domain, (2) at  $940 \pm 6$  Ma in the Mollendo area of the Camaná–Mollendo domain; (3) between *ca.* 1000 and 840 Ma in the Atico domain. This evidence suggests that in the Arequipa

Massif metamorphic domains are juxtaposed that underwent Grenvillian metamorphism at different times and had different cooling histories.

It is difficult to distinguish the effects of the Grenvillian metamorphic overprint on the older UHT paragenesis. Martignole and Martelat (2003), although favouring a single metamorphism of Grenville-age, leave this question open, suggesting that this might correspond to the lowest-*P* event ( $T < 900$  °C) they recognized. In our hypothesis that the UHT metamorphism in Arequipa was Paleoproterozoic, temperatures attained during Grenvillian metamorphism had to be high enough to completely reset the Th–U–Pb system in monazites (*ca.* 730 °C; Copeland et al., 1988; Parrish, 1990) unless the monazite formed only during the Grenvillian event. Moreover Grenville-age Ms-pegmatites are evidence for renewed partial melting at this time. High-grade metamorphic conditions were thus probably attained during Grenvillian metamorphism in the Camaná–Mollendo domain. In the Atico domain however, Grenvillian metamorphism only attained *P–T* values within the stability field of staurolite + andalusite (Shackleton et al., 1979) implying a low-pressure type of metamorphism.

### 8.4. Paleozoic events: the Ordovician magmatic arc

Ordovician crystallization ages found here for the igneous protoliths of the Ilo domain were unexpected. Martignole et al. (2005) interpreted these rocks as a Grenvillian AMG (anorthosite–mangerite–charnockite–granite) suite on the basis of locally preserved relict high-temperature minerals such as pyroxenes and alleged metamorphic garnet, and Nd model ages of *ca.* 1.15 Ga. In our samples those minerals are absent. However minerals such as hornblende, biotite and rutile (in anorthosite) are preserved in the less retrogressed rocks (ILO-20 and ILO-23) and also argue in favour of an earlier high-temperature history including igneous crystallization in a deep magma chamber and metamorphism. The latter, which is evidenced by zircon overgrowths on igneous cores (e.g., ILO-20), took place within the analytical uncertainty of the crystallization ages. Ages of igneous zircons of *ca.* 460 Ma place this magmatism within the Famatinian orogenic cycle, well-known in NW Argentina, which took place along the proto-Andean margin of Gondwana (Pankhurst et al., 2000; Dahlquist et al., 2008, and references therein). Loewy et al. (2004) obtained U–Pb ages between 440 and 468 Ma for late granitic intrusions in the Arequipa Massif. Nd isotope composition (Table 2) suggest that the Ilo magmatism involved variable contamination with an evolved continental crust ( $\epsilon_{\text{Nd}} = -3.6$  to  $-7.8$ ;  $T_{\text{DM}} = 1.5$  to 1.8 Ga) with some evidence for mixing/mingling between magmas.

A Paleozoic metamorphic event is also recorded in the San Juan Marcona domain. Here (sample MAR-8), an event that produced variable Pb-loss of Grenvillian and Paleoproterozoic zircon is suggested by a discordia with a lower intercept at  $469 \pm 70$  Ma. Strong retrogression in the San Juan Marcona and Ocoña areas was attributed by Loewy et al. (2004) to an M3 tectonothermal event at *ca.* 465 Ma, i.e., Ordovician, as inferred from the U–Pb ages of alleged pre- and post-metamorphic plutons in the area. This event correlates with the Marcona event of Shackleton et al. (1979), which produced a foliation (S3) and greenschist-facies retrogression of the basement gneisses. The Ocoña phyllonite zone that separates the Atico domain from the Camaná–Mollendo domain was attributed to this M3–S3 event (Shackleton et al., 1979; Loewy et al., 2004).

In the Ilo domain, zircons from the mylonitic dark gneiss and mylonitic porphyritic granite record evidence of overprinting at 430–440 Ma that could be related to retrogression within the shear zone. This age is within error of that found at San Juan Marcona

and attests to metamorphic processes in Ordovician to Silurian times. This Ordovician to Silurian low-grade metamorphic overprint was largely restricted to shear zones and basement areas near the contact with cover sequences of Neoproterozoic age, such as in the San Juan Marcona domain (Shackleton et al., 1979; Chew et al., 2007). Focused flow of water-rich fluids along these zones played a significant role in metamorphism. Large areas of the Arequipa Massif, however, do not record any evidence of Paleozoic metamorphism.

### 8.5. Correlations and geodynamic implications

There is agreement that the Laurentian and Amazonian cratons were juxtaposed across the Grenvillian orogenic belt at the end of Rodinia amalgamation at ca. 1.0 Ga (e.g., Dalla Salda et al., 1992; Dalziel, 1994, 1997; Sadowski and Bettencourt, 1996; Sadowski, 2002; Loewy et al., 2003; Tohver et al., 2004; Li et al., 2008). Models differ however on the relative position of these cratons, either in the NE (relative to present-day North America) or in the SE. Fig. 7 shows a paleomagnetically-constrained paleogeography at ca. 1.2 Ga, i.e., the alleged age of collision across the Grenville-age Sunsás orogen, according to Tohver et al. (2004). It shows the location of the Grenville belt of North America and its alleged counterpart along the western and southwestern margin of Amazonia, together with outcrops of basement in the Central Andes region with Grenvillian ages of interest to this contribution.

The Arequipa Massif is a Paleoproterozoic inlier overprinted by the Grenvillian orogeny. Correlation with other Paleoproterozoic terranes is hindered by the isolation of the Arequipa Massif. Compared with the ages of Paleoproterozoic orogenies in Laurentia (e.g., Goodge and Vervoort, 2006, fig. 1; Goodge et al., 2004, fig. 16) the age range of 1.76–2.1 Ga of Paleoproterozoic zircon in the San Juan and Camaná–Mollendo domains embraces the Yavapai orogeny (1.7–1.8 Ga) and the Penokean and Trans-Hudson orogenies (1.8–2.0 Ga; Schulz and Cannon, 2007; Whitmayer and Karlstrom, 2007). If formerly part of Laurentia, the Arequipa Massif would be a relic of the pre-Grenvillian southern margin of the continent (present coordinates) isolated from the northern Paleoproterozoic belts by younger juvenile accretionary belts (Mazatzal and the Granite-Rhyolite province: 1.7–1.3 Ga; Fig. 7). The Laurentian connection was initially favoured by Dalziel (1992, 1994) and Sadowski and Bettencourt (1996, and references therein), whereas Loewy et al. (2003) suggested an alternative source in the Kalahari craton. Rocks of equivalent age are also found in the Ventuari–Tapajós belt of the Amazonian craton (2.0–1.8 Ga; Cordani and Teixeira, 2007), although the latter is a juvenile accretionary belt whilst the Arequipa Massif is a block of reworked continental crust. Moreover the Ventuari–Tapajós belt is quite distant from the Arequipa Massif in current reconstructions, which would imply a significant lateral displacement before Grenvillian metamorphism. Irrespective of the cratonic source it is commonly accepted that the Arequipa Massif lay between Laurentia and Amazonia in Rodinia (e.g., Cordani et al., 2005b; Ramos, 2008).

The Rio Apa block, south of present-day Amazonia (Fig. 7), is another area to be considered, with U–Pb SHRIMP zircon ages largely coincident with those of detrital zircons in the Arequipa migmatitic gneisses (Cordani et al., 2008). Here widespread granitoid gneisses (1.94 Ga) were intruded by granitic plutons of the Alumiador Intrusive Suite (ca. 1.83 Ga) and younger orthogneisses were formed between 1.7 and 1.76 Ga. Nd model ages are between 2.2 and 2.53 Ga (Cordani et al., 2005a). Allegedly Paleoproterozoic metamorphism was medium- to high-grade (Cordani et al., 2008), but so far no evidence of UHT metamorphism has been recorded. The Rio Apa block was overprinted by a thermal event at ca. 1.3 Ga (Cordani et al., 2005a), i.e., at the end of the Rondonian–San Ignacio orogenies (e.g., Böger et al., 2005; Cordani and

Teixeira, 2007) and together with the Arequipa Massif could thus be part of a larger Paleoproterozoic craton accreted to Amazonia at a still uncertain time, probably 1.3 Ga or earlier. The Maz domain in the Western Sierras Pampeanas of Argentina contains metasedimentary rocks with Paleoproterozoic zircons (1.7–1.9 Ga) and old Nd model ages (1.7–2.7 Ga), and was also reworked by the Grenvillian orogeny (Casquet et al., 2008), so that it could also be part of the same continental block (Casquet et al., 2009).

Accretion of the Arequipa Massif to Amazonia was attributed to the Grenville-age Sunsás orogeny by Loewy et al. (2004). Grenvillian ages of igneous rocks and metamorphism were early recognized along the southeastern margin of the Amazonian craton by Priem et al. (1971) and Litherland et al. (1989, and references therein). The latter authors coined the name Sunsás orogeny for this tectonothermal event and attributed to it an age of 1000–950 Ma on the basis of Rb–Sr and K–Ar dating. Orogeny involved shearing, folding and metamorphism along discrete belts that wrap around an older metamorphic core, the Paraguá block (ca. 1.7 Ga; Böger et al., 2005), overprinted in turn by the Rondonian–San Ignacio orogenies between 1.5 and 1.3 Ga (Sadowski and Bettencourt, 1996; Cordani and Teixeira, 2007). Tohver et al. (2005) summarized the Grenvillian history as consisting of two events, an older one of alleged Laurentia–Amazonia collision (1.2–1.12 Ga; U/Pb and  $^{39}\text{Ar}/^{40}\text{Ar}$  metamorphic ages), and a younger one of intracontinental strike-slip motion at ca. 1.1. The second event (Sunsás–Aguapei–Nova Brasilândia orogeny) was also accompanied by magmatism and metamorphism. Metamorphism was mostly of low-grade but reached granulitic facies at Nova Brasilândia, dated at 1.09 Ga with cooling through 920 Ma. Precise U–Pb SHRIMP ages led Boger et al. (2005) to constrain Sunsás contractional deformation as predating ca. 1070 Ma. Santos et al. (2008) revisited the tectonic evolution of the southern margin of Amazonia and re-interpreted the Sunsás orogeny as an autochthonous orogen involving four orogenic pulses between 1465 and 1110 Ma, suggesting a Laurentia–Amazonia connection at ca. 1450 Ma. In any case, the period between 1070 Ma and ca. 980 Ma was apparently a period of craton stabilization, with anorogenic granitic magmatism along the southern margin of Amazonia (Santos et al., 2008; Cordani and Teixeira, 2007, and references therein).

In the Grenville province of Canada the Grenvillian orogeny embraces rocks and events with ages between ca. 1.3 and 0.95 Ga (Davidson, 1995; Bartholomew and Hatcher, this volume). Between 1100 and ca. 980 Ma two contractional episodes were considered by Rivers (2008, and references therein) as distinct from older orogenic events and the only representatives of the Grenvillian orogeny: the widespread penetrative Ottawa orogenic phase (1090–1020 Ma) and the Rigolet event (ca. 1000–980 Ma). Rivers (2008) argued that collapse of the Ottawa orogen, thickened as a result of probable Laurentia–Amazonia collision, took place during the time interval 1050–1020. Former contractional structures were reworked in this extensional phase and AMGC complexes were intruded that heated the middle crust. Horst-and-graben structures developed at this time in the upper crust. During the time interval 1020–950 Ma the Grenville province underwent renewed contraction, focused mainly within the Parautochthonous Belt near the Grenville front. The hinterland however underwent protracted extensional collapse over this period with development of extensional shear zones, deep ductile detachments and medium-low pressure metamorphism (Rivers, 2008).

The contractional phase of the Ottawa orogeny (1090–1050 Ma) (time equivalent of the Sunsás orogeny) and the older orogenic events long known in the Grenville province of Canada, i.e., the Elzevirian and the Shawinigan orogenies are not recognized in the Arequipa Massif. However, the coincidence of the Arequipa Massif metamorphic ages of 1040–840 Ma with protracted extension both in the Laurentian Grenville and in southern Amazonia

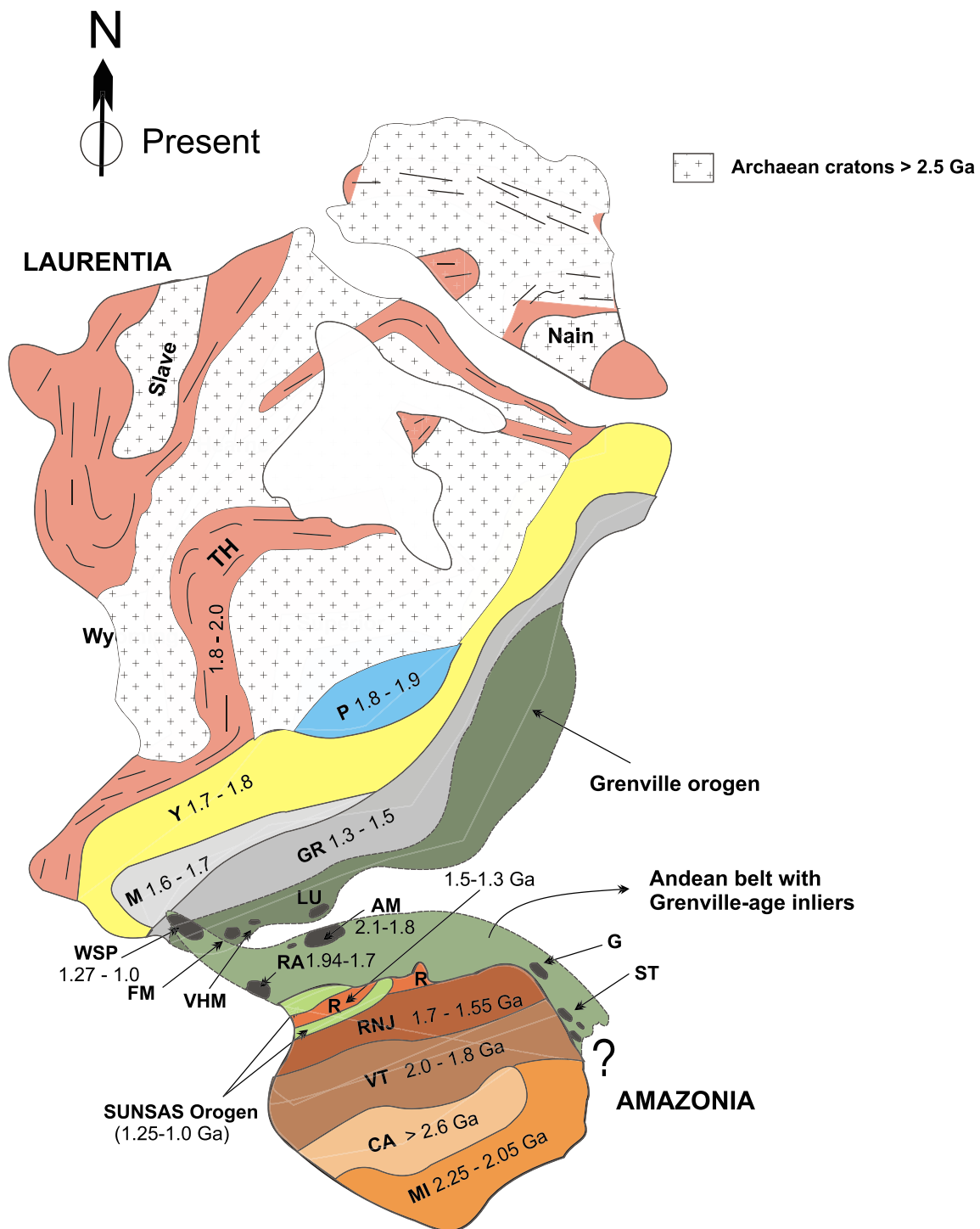


**Fig. 7.** Paleogeographical reconstruction of Laurentia and Amazonia at ca. 1.2 Ga (Tohver et al., 2004), showing Precambrian orogenic belts with ages according to Goodge et al. (2004, fig. 16), Tohver et al. (2004) and Cordani and Teixeira (2007) (Laurentia in its present position). Outcrops of basement with Grenvillian ages in southern Laurentia and in the Central Andean region (Peru, NW Chile and Argentina) have been included (the latter in its present position relative to Amazonia). Laurentia: TH, Trans-Hudson and related mobile belts; P, Penokean orogen; Y, Yavapai orogen; M, Mazatzal orogen; GR, Granite-Rhyolite province; FM, Franklin mountains outcrop; VHM, Van Horn Mountains outcrop; LU, Llano Uplift outcrop. Amazonia: MI, Maroni–Itacaiunas Province; CA, Central Amazonia province; VT, Ventuari–Tapajós province; RNJ, Rio Negro Juruena province; R, Rondonian–San Ignacio province; Sunsás, orogenic belts of Grenvillian age along southern Amazonia; AM, Arequipa Massif (Peru); RA, Rio Apa outcrop (Brasil, Paraguay); WSP, Western Sierras Pampeanas (Argentina); G, Garzón Massif (Colombia); ST, Santander Massif (Colombia).

suggests that metamorphism in Arequipa, which was of low-*P* type, might be related to overall extension and heating, and not to contraction as formerly thought. The precise tectonic setting remains unknown and more structural work is required to constrain it. Laurentia–Amazonia collision took probably place earlier, either at ca. 1.2 Ga (Tohver et al., 2005) or later during the Ottawan (Sunsás) orogeny (Rivers, 2008) but is not recognized in the Arequipa

Massif except for the detrital zircons of 1200–1260 Ma in the Atico metasedimentary rocks. Whether formerly part of Laurentia or of Amazonia, or other, the location of Arequipa before collision remains uncertain.

The Atico sedimentary basin that formed between 1200 and 1000 Ma might be also related to the protracted extensional event referred to above, or it could be a foreland basin resulting from

Laurentia – Amazonia collision. The magmatism at Ilo that included anorthositic was not involved in the Grenvillian metamorphism. Grenvillian metamorphic domains with different  $P$ – $T$ – $t$  histories were probably juxtaposed across low-grade shear zones in the Ordovician–Silurian during the contractional Famatinian orogeny.

## 9. Conclusions

The Arequipa Massif is a Paleoproterozoic inlier in the South American Grenville-age orogen. It was probably part of a larger continental block that also included the Río Apa block and the Western Sierras Pampeanas Maz terrane.

The Paleoproterozoic pattern that emerges is one of an orogeny between ca. 1.79 and 2.1 Ga (Orosirian to Rhyacian) involving: (a) early magmatism (between 1.89 and 2.1 Ga), presumably intruded through partly Archaean continental crust, (b) sedimentation of a thick sequence of terrigenous sediments, (c) UHT metamorphism at ca. 1.87 Ga, and (d) late felsic magmatism at ca. 1.79 Ga.

The Atico domain can be interpreted as a sedimentary basin deposited on a Paleoproterozoic high-grade basement consisting of igneous and metamorphic rocks. Deposition occurred between ca. 1200 and ca. 1000 Ma, i.e., in the Late-Mesoproterozoic. Detrital zircons were fed from a source area similar to the high-grade Camaná–Mollendo and San Juan domains, but also from an unknown source that provided Mesoproterozoic zircons of 1260–1600 Ma.

Grenville-age metamorphism at Arequipa took place in up to three stages: (1) ca. 1040 Ma in the Quilca and Camaná areas of the Camaná–Mollendo domain, and in the San Juan Marcona domain, (2)  $940 \pm 6$  Ma in the Mollendo area of the Camaná–Mollendo domain; (3) between 1000 and 850 Ma in the Atico domain. In the Arequipa Massif metamorphic domains are therefore juxtaposed that underwent different Grenvillian metamorphic histories. The geodynamic significance of Grenvillian metamorphism is unknown but it could be related to extension and not to collision as formerly argued.

During the Early Paleozoic the Arequipa Massif underwent magmatism at ca. 465 Ma and focused retrogression along shear zones or unconformities between 430 and 440 Ma.

## Acknowledgements

Financial support for this work was provided by Spanish MEC grant CGL2005-02065/BTE and Universidad Complutense grant 910495 and Argentinian PICT 1009. We are grateful to Instituto Geológico Minero y Metalúrgico (INGEMMET) of Perú, and particularly to Dr. Victor Carlotto, who helped us with the fieldwork.

## Appendix A. Supplementary data

Supplementary data associated with this article can be found, in the online version, at [doi:10.1016/j.jsames.2009.08.009](https://doi.org/10.1016/j.jsames.2009.08.009).

## References

- Arima, M., Gower, Ch.F., 1991. Osumilite-bearing granulites in the Eastern Grenville Province, Eastern Labrador, Canada: mineral parageneses and metamorphic conditions. *Journal of Petrology* 32 (1), 29–61.
- Black, L.P., Williams, I.S., Compston, W., 1986. Four zircon ages from one rock: the history of a 3930 Ma old granulite from the Mt. Stones, Enderby Land, Antarctica. *Contributions to Mineralogy and Petrology* 94, 427–437.
- Bock, B., Bahlburg, H., Wörner, G., Zimmermann, U., 2000. Tracing crustal evolution in the Southern Central Andes from Late Precambrian to Permian with geochemical and Nd and Pb data. *Journal of Geology* 108, 515–535.
- Böger, S.D., Raetz, M., Giles, D., Etchart, E., Fanning, C.M., 2005. U–Pb data from the Sunsás region of Eastern Bolivia, evidence for an allochthonous origin of the Paragua block. *Precambrian Research* 139, 121–146.
- Carson, C.J., Ague, J.J., Coath, C.D., 2002. U–Pb geochronology from Tonagh Island, East Antarctica: implications for the timing of ultra-high temperature metamorphism of the Napier complex. *Precambrian Research* 116, 237–263.
- Casquet, C., Pankhurst, R.J., Rapela, C., Galindo, C., Fanning, C.M., Chiaradia, M., Baldo, E., González-Casado, J.M., Dahlquist, J.A., 2008. The Maz terrane: a Mesoproterozoic domain in the Western Sierras Pampeanas (Argentina) equivalent to the Arequipa–Antofalla block of southern Peru? Implications for Western Gondwana margin evolution. *Gondwana Research* 13, 163–175.
- Casquet, C., Rapela, C.W., Pankhurst, R.J., Baldo, E., Galindo, C., Saavedra, J., Fanning, C.M., 2009. Paleoproterozoic terranes in southern South America: accretion to Amazonia, involvement in Rodinia formation and further W. Gondwana accretion. In: *Fermor Meeting: Rodinia: Supercontinents, Superplumes and Scotland*, Edinburgh, Abstract.
- Chew, D.M., Schaltegger, U., Kosler, J., Whitehouse, M.J., Gutjahr, M., Spikings, R.A., Miskovic, A., 2007. U–Pb geochronologic evidence for the evolution of the Gondwanan margin of the north-central Andes. *Geological Society of America Bulletin* 119, 697–711.
- Cobbing, E.J., Pitcher, 1972. Plate tectonics and the Peruvian Andes. *Nature* 246, 51–53.
- Cobbing, E.J., Ozard, J.M., Snelling, N.J., 1977. Reconnaissance geochronology of the crystalline basement of the Coastal Cordillera of southern Peru. *Geological Society of America Bulletin* 88, 241–246.
- Copeland, P., Parrish, R.R., Harrison, T.M., 1988. Identification of inherited radiogenic Pb in monazite and its implications for U–Pb systematics. *Nature* 333, 760–763.
- Cordani, U.G., Teixeira, W., 2007. Proterozoic accretionary belts in the Amazonian craton. In: Hatcher, R.D., Jr., Carlson, M.P., McBride, J.H., Martínez Catalán, J.R. (Eds.), *4-D Framework of Continental Crust*, vol. 200. Geological Society of America, Memoir, pp. 297–320.
- Cordani, U.G., Tassinari, C.C.G., Reis Rolim, D.R., 2005a. The basement of the Rio Apa craton in Mato Grosso do Sul (Brazil) and Northern Paraguay: a geochronological correlation with tectonic provinces of the south-western Amazonian Craton. In: Pankhurst, R.J., Veiga, G.D. (Eds.), *Gondwana 12: Geological and Biological Heritage of Gondwana*. Abstracts. Academia Nacional de Ciencias, Córdoba, Argentina, p. 113.
- Cordani, U.G., Cardona, A., Jimenez, D.M., Liu, D., Nutman, A.P., 2005b. Geochronology of Proterozoic basement inliers in the Colombian Andes: tectonic history of remnants of a fragmented Grenvillian belt. In: Vaughan, A.P.M., Leat, P.T., Pankhurst, R.J. (Eds.), *Terrane Processes at the Margins of Gondwana*, vol. 246. Geological Society, London, pp. 329–346. Special Publication.
- Cordani, U.G., Tassinari, C.C.G., Teixeira, W., Coutinho, J.M.V., 2008. U–Pb SHRIMP zircon ages for the Rio Apa cratonic fragment in Mato Grosso do Sul (Brazil) and northern Paraguay: tectonic implications. In: *VI South American Symposium on Isotope Geology*, Bariloche, Argentina, Proceedings.
- Corfu, F., Hanchar, J.M., Hoskin, W.O., Kinny, P., 2003. Atlas of Zircon Textures. In: Hanchar, J.M. and Hoskin, P.W.O. (Eds.), *Zircon, Reviews in Mineralogy and Geochemistry*, 53, 469–500.
- Dahlquist, J.A., Pankhurst, R.J., Rapela, C.W., Galindo, C., Alasino, P., Fanning, C.M., Saavedra, J., Baldo, E., 2008. New SHRIMP U–Pb data from the Famatina complex: constraining Early–Mid Ordovician Famatinian magmatism in the Sierras Pampeanas, Argentina. *Geologica Acta* 6, 319–333.
- Dalla Saldá, L.H., Dalziel, I.W.D., Cingolani, C.A., Varela, R., 1992. Did the Taconic Appalachians continue into southern South America? *Geology* 20, 1059–1062.
- Dalmayrac, B., Lancelot, J.R., Leyreloup, A., 1977. Two-billion year granulites in the Late Precambrian metamorphic basement along the southern Peruvian coast. *Science* 198, 49–51.
- Dalziel, I.W.D., 1992. On the organization of American plates in the Neoproterozoic and the breakout of Laurentia. *GSA Today* 2, 1–2.
- Dalziel, I.W.D., 1994. Precambrian Scotland as a Laurentia–Gondwana link: origin and significance of cratonic promontories. *Geology* 22, 589–592.
- Dalziel, I.W.D., 1997. Overview. Neoproterozoic–Paleozoic geography and tectonics: review, hypothesis, environmental speculation. *Geological Society of America Bulletin* 109, 16–42.
- Davidson, A., 1995. A review of the Grenville orogen in its North American type area. *Journal of Australian Geology and Geophysics* 16, 3–24.
- DePaolo, D.J., 1981. Neodymium isotopes in the Colorado Front Range and crust–mantle evolution in the Proterozoic. *Nature* 291, 193–196.
- DePaolo, D.J., Linn, A.M., Schubert, G., 1991. The continental crustal age distribution: methods of determining mantle separation ages from Sm–Nd isotopic data and application to the Southwestern United States. *Journal of Geophysical Research* B96, 2071–2088.
- Goode, J.W., Vervoort, J.D., 2006. Origin of Mesoproterozoic A-type granites in Laurentia: Hf isotope evidence. *Earth and Planetary Science Letters* 243, 711–731.
- Goode, J.W., Fanning, M., Bennett, V.C., 2001. U–Pb evidence of 1.7 Ga crustal tectonism during the Nimrod orogeny in the Transantarctic Mountains, Antarctica: implications for Proterozoic plate reconstructions. *Precambrian Research* 112, 261–288.
- Goode, J.W., Williams, I.S., Myrow, P., 2004. Provenance of Neoproterozoic and lower Paleozoic siliciclastic rocks of the Central Ross orogen, Antarctica: detrital record of rift-, passive-, and active-margin sedimentation. *Geological Society of America Bulletin* 116, 1253–1279.
- Hoffman, P.F., 1991. Did the breakout of Laurentia turn Gondwanaland inside out? *Science* 252, 1409–1412.
- Li, Z.X., Bogdanova, S.V., Collins, A.S., Davidson, A., De Waele, B., Ernst, R.E., Fitzsimons, I.C.W., Fuck, R.A., Gladkochub, D.P., Jacobs, J., Karlstrom, K.E., Lu, S.,

- Natapov, Pease, V., Pisarevsky, S.A., Thrane, K., Vernikovskiy, V., . Assembly, configuration, and break-up history of Rodinia: a synthesis. *Precambrian Research* 160, 179–210.
- Litherland, M., Annells, R.N., Darbyshire, D.P.F., Fletcher, C.J.N., Hawkins, M.P., Klinck, B.A., Mitchell, W.I., ÓConnor, E.A., Pitfield, P.E.J., Power, G., Webb, B.C., 1989. The Proterozoic of Eastern Bolivia and its relationships to the Andean mobile belt. *Precambrian Research* 43, 157–174.
- Loewy, S.L., Connelly, J.N., Dalziel, I.W.D., Gower, C.F., 2003. Eastern Laurentia in Rodinia: constraints from whole-rock Pb and U/Pb geochronology. *Tectonophysics* 375, 169–197.
- Loewy, S.L., Connelly, J.N., Dalziel, I.W.D., 2004. An orphaned block: the Arequipa–Antofalla basement of the Central Andean margin of South America. *Geological Society of America Bulletin* 116, 171–187.
- Ludwig, K.R., 2001. SQUID 1.02. A users manual. Berkeley Geochronological Center Special Publication, 2, 2455 Ridge Road, Berkeley, CA 94709, USA.
- Martignole, J., Martelat, J.E., 2003. Regional-scale Grenvillian-age UHT metamorphism in the Mollendo–Camaná block (basement of the Peruvian Andes). *Journal of Metamorphic Geology* 21 (1), 99–120.
- Martignole, J., Stevenson, R., Martelat, J.E., 2005. A Grenvillian Anorthosite–Mangerite–Charnockite–Granite Suite in the Basement of the Andes: the Ilo AMCG Site (Southern Peru). *IDSAG, Barcelona*, pp. 481–484 (Extended Abstracts).
- Moore, E.M., 1991. Southwest US–East Antarctic (SWEAT) connection: a hypothesis. *Geology* 19, 425–428.
- Pankhurst, R.J., Rapela, C.W., Fanning, C.M., 2000. Age and origin of coeval TTG, I- and S-type granites in the Famatinian belt of NW Argentina. *Transactions of the Royal Society of Edinburgh: Earth Sciences* 91, 151–168.
- Parrish, R.R., 1990. U–Pb dating of monazite and its application to geological problems. *Canadian Journal Earth Sciences* 27, 1431–1450.
- Priem, H.N.A., Boelrijk, N.A.I.M., Hebeda, E.H., Verdumen, E.A.T., Verschure, R.H., Bon, E.H., 1971. Granitic complexes and associated tin mineralization of Grenville age in Rondonia, Western Brasil. *Geological Society of America Bulletin* 82 (4), 1095–1102.
- Ramos, V.A., 1988. Late Proterozoic – Early Paleozoic of South America – a collisional history. *Episodes* 11, 168–174.
- Ramos, V.A., 2008. The basement of the Central Andes: the Arequipa and related terranes. *Annual Review of Earth and Planetary Sciences* 36, 289–324.
- Restrepo-Pace, P.A., Ruiz, J., Gehlers, G., Cosca, M., 1997. Geochronology and Nd isotopic data of Grenville-age rocks in the Colombian Andes: new constraints from Late Proterozoic – Early Paleozoic paleocontinental reconstructions of the Americas. *Earth and Planetary Science Letters* 150, 427–441.
- Rivers, 2008. Assembly and preservation of lower, mid and upper orogenic crust in the Grenville Province – implications for the evolution of large hot long-duration orogens. *Precambrian Research* 167, 237–259.
- Sadowski, G.R., 2002. The fit between Amazonia, Baltica and Laurentia during Mesoproterozoic assemblage of the supercontinent Rodinia. *Gondwana Research* 5, 101–107.
- Sadowski, G.R., Bettencourt, J.S., 1996. Mesoproterozoic tectonic correlations between Eastern Laurentia and the western border of the Amazon craton. *Precambrian Research* 76, 213–227.
- Santos, J.O.S., Rizzotto, G.J., Potter, P.E., McNaughton, N.J., Matos, R.S., Hartmann, L.A., Chemale Jr., F., Quadros, M.E.S., 2008. Age and autochthonous evolution of the Sunsás orogen in West Amazon craton based on mapping and U–Pb geochronology. *Precambrian Research* 165, 120–152.
- Schulz, K.L., Cannon, W.F., 2007. The Penokean orogeny in the Lake Superior region. *Precambrian Research* 157, 4–25.
- Shackleton, R.M., Ries, A.C., Coward, M.P., Cobbold, P.R., 1979. Structure, metamorphism and geochronology of the Arequipa massif of Coastal Peru. *Journal of the Geological Society, London* 136, 195–214.
- Siivola, J., Schmid, R., 2007. List of mineral abbreviations. In: Fettes, D., Desmons, J. (Eds.), *Metamorphic Rocks. A Classification and Glossary of Terms*. Cambridge University Press, pp. 93–110.
- Taylor, S.R., McLennan, S.M., 1988. The significance of the rare earths in geochemistry and cosmochemistry. In: Gschneider, K.A., Jr., Eyring, L. (Eds.), *Handbook of the Physics and Chemistry of Rare Earths*, vol. 11. Elsevier Publications B.V., pp. 486–578.
- Tohver, E., Bettencourt, J.S., Tosdal, R., Mezger, K., Leite, W.B., Payolla, B.L., 2004. Terrane transfer during Grenville orogeny: tracing the Amazonian ancestry of southern Appalachian basement through Pb and Nd isotopes. *Earth and Planetary Science Letters* 228, 161–176.
- Tohver, E., van der Pluijm, B.A., Mezger, K., Scandolaria, J.E., Essene, E.J., 2005. Two stage tectonic history of the SW Amazon craton in the late Mesoproterozoic: identifying a cryptic suture zone. *Precambrian Research* 137, 35–59.
- Tosdal, R.M., 1996. The Amazon–Laurentian connection as viewed from the Middle Proterozoic rocks in the Central Andes, Western Peru and Northern Chile. *Tectonics* 15, 827–842.
- Vavra, G., Schmid, R., Gebauer, D., 1999. Internal morphology, habit and U–Th–Pb microanalysis of amphibolite-to-granulite facies zircons: geochronology and the Ivrea Zone (southern Alps). *Contributions to Mineralogy and Petrology* 134, 380–404.
- Wasteneys, H.A., Clark, A.H., Farrar, E., Langridge, R.J., 1995. Grenvillian granulite-facies metamorphism in the Arequipa Massif, Peru: a Laurentia–Gondwana link. *Earth and Planetary Science Letters* 132, 63–73.
- Whitmayer, S.J., Karlstrom, K.E., 2007. Tectonic model for the Proterozoic growth of North America. *Geosphere* 3, 220–259.
- Williams, I.S., 1998. U–Th–Pb geochronology by ion microprobe. In: McKibben, M.A., Shanks, W.C. III, Ridley, W.I. (Eds.), *Applications of Microanalytical Techniques to Understanding Mineralizing Processes*. Reviews of Economic Geology, 7, 1–35.